



Key Points:

- We identified the source faults of 14 large earthquakes along the East Anatolian and northern Dead Sea fault systems
- Maximum magnitude for the East Anatolian Fault (EAF) zone is approximately 8.2
- Continental transforms may be described as having a collective memory

Supporting Information:

Supporting Information may be found in the online version of this article.

Correspondence to:

S. Carena,
sara.carena@lmu.de

Citation:

Carena, S., Friedrich, A. M., Verdecchia, A., Kahle, B., Rieger, S., & Kübler, S. (2023). Identification of source faults of large earthquakes in the Turkey-Syria border region between 1000 CE and the present, and their relevance for the 2023 M_w 7.8 Pazarcık earthquake. *Tectonics*, 42, e2023TC007890. <https://doi.org/10.1029/2023TC007890>

Received 17 APR 2023
Accepted 7 NOV 2023

Author Contributions:

Conceptualization: S. Carena, A. M. Friedrich
Formal analysis: S. Carena
Methodology: S. Carena, A. M. Friedrich
Resources: A. Verdecchia, S. Rieger, S. Kübler
Validation: A. M. Friedrich, A. Verdecchia
Visualization: S. Carena, A. M. Friedrich, B. Kahle
Writing – original draft: S. Carena, A. M. Friedrich
Writing – review & editing: S. Carena, A. Verdecchia, B. Kahle

© Wiley Periodicals LLC. The Authors. This is an open access article under the terms of the [Creative Commons Attribution License](https://creativecommons.org/licenses/by/4.0/), which permits use, distribution and reproduction in any medium, provided the original work is properly cited.

Identification of Source Faults of Large Earthquakes in the Turkey-Syria Border Region Between 1000 CE and the Present, and Their Relevance for the 2023 M_w 7.8 Pazarcık Earthquake

S. Carena¹ , A. M. Friedrich¹, A. Verdecchia² , B. Kahle^{1,3}, S. Rieger¹, and S. Kübler¹

¹Department of Earth and Environmental Sciences, Ludwig-Maximilians-Universität München, Munich, Germany, ²Institute for Geology, Mineralogy and Geophysics, Ruhr-Universität Bochum, Bochum, Germany, ³Department of Geological Sciences, University of Cape Town, Cape Town, South Africa

Abstract The 6 February 2023, M_w 7.8 Pazarcık earthquake in the Turkey-Syria border region raises the question of whether such a large earthquake could have been foreseen, as well as what is the maximum possible magnitude (M_{max}) of earthquakes on the East Anatolian Fault (EAF) system and on continental transform faults in general. To answer such questions, knowledge of past earthquakes and of their causative faults is necessary. Here, we integrate data from historical seismology, paleoseismology, archeoseismology, and remote sensing to identify the likely source faults of fourteen $M_w \geq 7$ earthquakes between 1000 CE and the present in the region. We find that the 2023 Pazarcık earthquake could have been foreseen in terms of location (the EAF) and timing (an earthquake along this fault was if anything overdue), but not magnitude. We hypothesize that the maximum earthquake magnitude for the EAF is in fact 8.2, that is, a single end-to-end rupture of the entire fault, and that the 2023 Pazarcık earthquake did not reach M_{max} by a fortuitous combination of circumstances. We conclude that such unusually large events are hard to model in terms of recurrence intervals, and that seismic hazard assessment along continental transforms cannot be done on individual fault systems but must include neighboring systems as well, because they are not kinematically independent at any time scale.

Plain Language Summary On 6 February 2023, there was a magnitude 7.8 earthquake in the Turkey-Syria border region. It surprised many people, including many Earth scientists, because of where it happened (on the East Anatolian fault [EAF]) and because of how large it was. People wondered whether it could have been foreseen, and how large an earthquake on this fault can really be. To figure this out, we looked at the history of earthquakes in the region in the last 1,000 years. We used information from historical seismology, paleoseismology, archeoseismology, and remote sensing to identify the faults that caused 14 earthquakes with magnitude 7 or greater in this region. We found that the location (EAF) and timing (it was due any time) of the 2023 earthquake were foreseeable, but not the magnitude. In fact, we believe that the maximum magnitude for the EAF is 8.2, and that the 2023 earthquake was below this maximum just by accident. It is hard to say how often such large events can happen, because many different things need to align. We also believe that it is necessary to look at neighboring fault systems when estimating seismic hazards, because they interact.

1. Introduction

The occurrence of the 6 February 2023 M_w 7.8 Pazarcık earthquake surprised not only the public, but also a large part of the geoscience community, due to the event size and location. This earthquake ruptured ~310 km of the left-lateral East Anatolian Fault (EAF) between Antakya and Çelikhan (Figure 1), which is ~55% of its length. It also ruptured through multiple segment boundaries (Figure 2). The EAF had been, until February 2023, a plate boundary fault largely overlooked by the international community, with the great majority of works since about 1970 mainly dealing with the North Anatolian Fault (NAF) because of its proximity to Istanbul and of its higher level of seismic activity in the past century. Publications about the NAF are on average ~6 times more numerous than those about the EAF (Table 1). Even the most recent earthquake on the EAF, the 24 January 2020 Elâziğ M_w 6.8 event, received surprisingly little attention. As of July 2023, there were only 10 geoscience papers about this earthquake listed in Web of Science. For comparison, the 1999 Düzce earthquake along the NAF had 13 papers listed in the same database over the first 3 years after the event, even though publishing rates have increased rapidly over time.

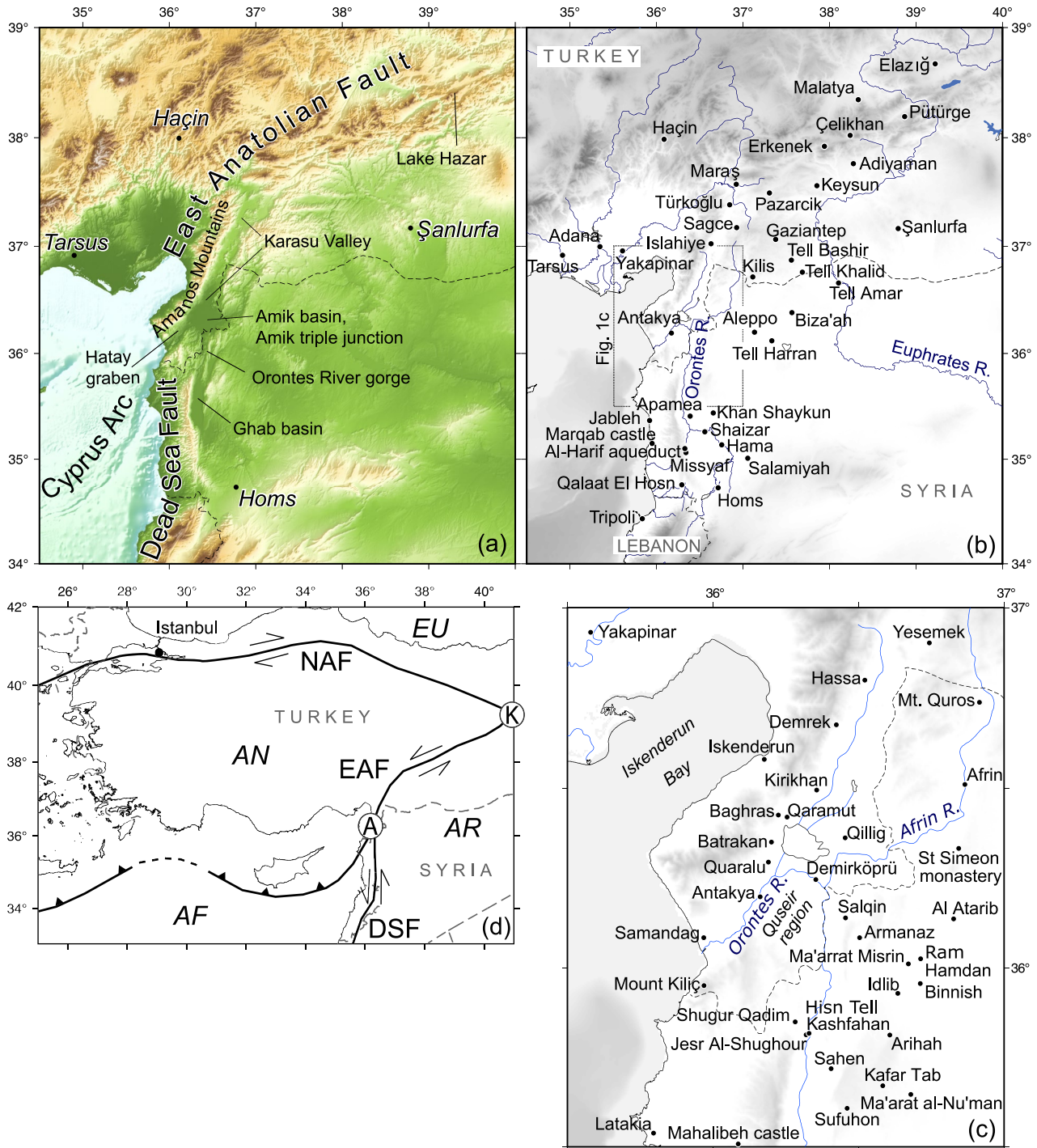


Figure 1. Location maps. Basic figures made with Generic Mapping Tools (Wessel et al., 2019), then modified. Topographic base is the SRTM 15 arc second global relief (Tozer et al., 2019). All maps: Mercator projection, WGS84 datum. All locality names in (b) and (c), with alternate forms, can be found in Table B1 and Data Set S1. NAF, North Anatolian Fault; EAF, East Anatolian Fault; DSF, Dead Sea Fault; K, Karliova triple junction; A, Amik triple junction; AF, African plate; AN, Anatolian plate; AR, Arabian plate; EU, Eurasian plate.

The EAF, however, has been documented as seismically very active in historical records, with magnitudes above 7.0 inferred for multiple earthquakes around the EAF in the past 1,000 years (e.g., Ambraseys, 1989, 2009; Guidoboni & Comastri, 2005; Meghraoui, 2015; Sbeinati et al., 2005). For most of these earthquakes, though,

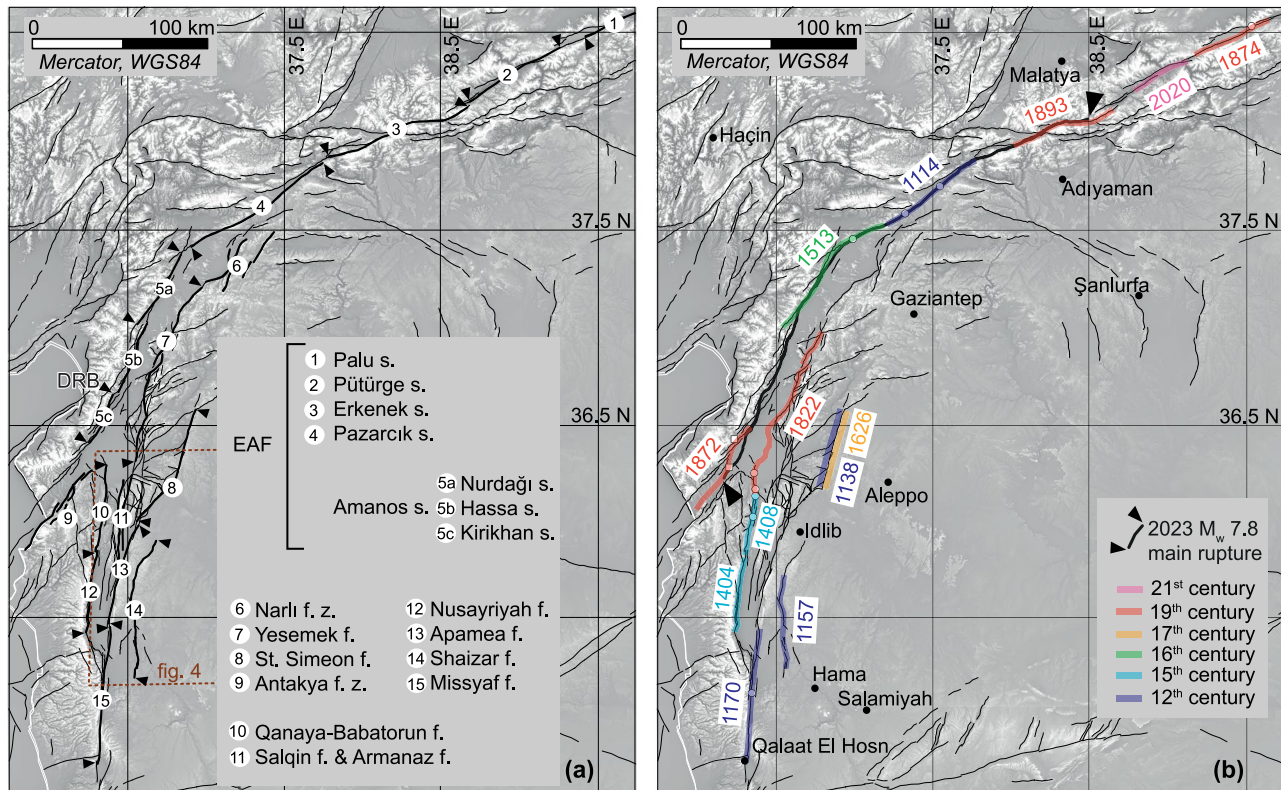


Figure 2. (a) Fault names (see Appendix B for details). The Amanos segment of the East Anatolian Fault (EAF) is split into three further segments. Except for the Demrek restraining bend (DRB), bends and stepovers are not labeled here because we do not refer to them; their names can be found in Duman and Emre (2013). s., segment; f., fault; f. z., fault zone. (b) Fault rupture/earthquake pairs from Table 2. Base map and other elements are described and referenced in Figure 3. Original uninterpreted base map included as Data Set S1, and ruptures as Data Set S1.

the specific source faults were either not identified, or identification from different authors varies considerably, or it lacks documentation. Lack of knowledge of source faults precludes the calculation of fault slip rates and recurrence times, and the estimation of seismic hazards and M_{max} . It also precludes having a rigorous base for stress and strain modeling and for studying dynamic rupture propagation.

Our goal is therefore to systematically identify the most likely source of each large ($M_w \geq 7.0$) earthquake along the East Anatolian and Dead Sea fault systems between Lake Hazar in the north and Qalaat El Hosn, Syria, in the south (Figure 1) in the past $\sim 1,000$ years, because these earthquakes may have had a direct and significant influence on the timing, location, and size of the 2023 M_w 7.8 Pazarcık earthquake. The more recent an earthquake is, the more likely it is to have been the “last event” on its source fault, determining the last coseismic and postseismic stress changes associated with the fault itself. Before 1000 CE the historical records are in any case very fragmentary, making it impossible to associate most earthquakes with a specific fault. By integrating

Table 1

Mentions of “East Anatolian Fault” (EAF) Versus “North Anatolian Fault” (NAF) in the Title of Publications From Four Major Bibliographical Databases

| Source ^a | EAF | NAF | Ratio NAF/EAF | Time range ^b |
|---|-----|------|---------------|-------------------------|
| GeoRef | 120 | 951 | 7.9 | 1972 to October 2023 |
| Google Scholar | 238 | 1480 | 6.2 | 1969 to October 2023 |
| Scopus | 67 | 447 | 6.3 | 1975 to October 2023 |
| Web of Science Core Collection ^c | 74 | 385 | 5.2 | 1975 to October 2023 |

^aExcept for GeoRef, which is specific for geosciences, and Google Scholar, which cannot be filtered, the other two sources were filtered to include only geosciences-relevant fields. ^bStart time is the year of the first publication about either fault in the database. ^cFive of the EAF publications were added between April and October 2023, and concern the two 2023 major earthquakes.

Table 2
List of Earthquakes and Corresponding Source Faults

| Date ^a | M_w^b | Name ^a | Rupture length (km) ^b | Aftershocks (months) | Source fault or fault segment |
|-------------------|-----------|-----------------------|----------------------------------|----------------------|----------------------------------|
| 6 February 2023 | 7.8 | Pazarcık | ~310 | Ongoing | Amanos, Pazarcık, & Erkenek s. |
| 24 January 2020 | 6.8 | Elâziğ | (~35) | 19 ^c | Pütürge s. |
| 2 March 1893 | 7.2 ± 0.1 | Malatya | ~60 | >12 ^d | Erkenek s. |
| 14 January 1874 | 7.1 | Sarikamiş | ~45 | ≥12 ^f | Palu s. |
| 3 April 1872 | 7.2 | Amik Gölü | ~50 | 10 ^c | Kirikhan s. & Antakya f. z. |
| 13 August 1822 | 7.5 | Southeastern Anatolia | ~110 | 30 ^c | Yesemek f. & Qanaya-Babatorun f. |
| 21 January 1626 | 7.2 | Hama | ~50 | Unknown | northern St. Simeon f. |
| 1513/1514 | ≥7.4 | Malatya | ≥80 | Unknown | Pazarcık & Nurdağı s. |
| 29 December 1408 | 7.0 | Shugr-Bekas | ~40 | Unknown | Qanaya-Babatorun f. |
| 20 February 1404 | ≥7.0 | Aleppo | ≥40 | ≥9 ^{f,g} | Nusayriyah f. |
| 29 June 1170 | 7.3–7.4 | Shaizar | ~80 | 4 ^c | Missyaf f. |
| 12 August 1157 | 7.2 | Apamea | ~50 | 21 ^c | Shaizar f. |
| 11 October 1138 | 7.2 | Atharib | ~50 | 8 ^c | northern St. Simeon f. |
| 29 November 1114 | ≥7.2 | Antioch, Maraş | ≥50 | 5 ^f | Pazarcık s. |

^aAmbraseys (2009), except for events from 2020 (K. O. Çetin et al., 2020) and 2023 (U.S. Geological Survey, 2023). ^bFor most of the earthquakes, we have estimated surface rupture lengths based on Wells & Coppersmith (1994), unless lengths were reported in original sources (discussion in text). The magnitude reported here is our preferred one among the sources discussed in the text. For the Elâziğ earthquake the rupture length value is in brackets because it did not rupture at the surface, though it had shallow slip (Pousse-Beltran et al., 2020). ^cSalamon (2008). ^dSatılmış (2016). ^eÖztürk (2021). ^fAmbraseys (2009). ^gNot possible to really distinguish all aftershocks of 1404 from foreshocks of 1408.

historical records with paleoseismological ones in a tectonic context, we aim to identify a set of reasonable fault/earthquake pairs and any plausible alternatives that can be used for both modeling purposes and the identification of key field sites for further studies.

2. Method and Results

The identification by previous authors of source faults of historical earthquakes along the EAF and northern Dead Sea Fault zone (DSF) is patchy. The typical case is, for example, when a historical seismology work assigns an earthquake to a fault simply on the basis that it is a known active fault in the general epicentral area. Often the source faults identified in this way are then reported by later authors without any critical re-evaluation, even in those cases when the original author had clearly stated that they were just doing a “best guess” approach with no additional data. In most cases each work identifies one or two earthquake/source pairs, or identifies multiple earthquakes, but all on the same fault. Unfortunately, identifying source faults in isolation or without looking at all data available in both time and space is more likely to result in mis-identification, the more so the older the earthquake is. We have therefore started from published historical seismology works, re-evaluating each piece of information from different authors about the same earthquake, and combining this with data from paleoseismology and remote sensing (often more recent), following the approach suggested by Daëron et al. (2007) for future studies on the DSF. We have not developed new methods, software, or collected field data. Rather, we have carried out a comprehensive review of the information that already exists and attempted to weed out inconsistencies and integrate information from different fields. Finally, when reviewing information, we have done so for several earthquakes and faults simultaneously, when these are (or could be) in the same sub-region.

2.1. Identification of Source Faults

In the case of the Turkey-Syria border region, several of the faults have been trenched, so several events from the past 1,000 years can be assigned to a specific fault with a reasonable degree of confidence. In some cases, a couple of different options are equally plausible but, overall, there is a limited combination of possible earthquake/source-fault pairs, because there is only a limited number of faults in the area that are long enough

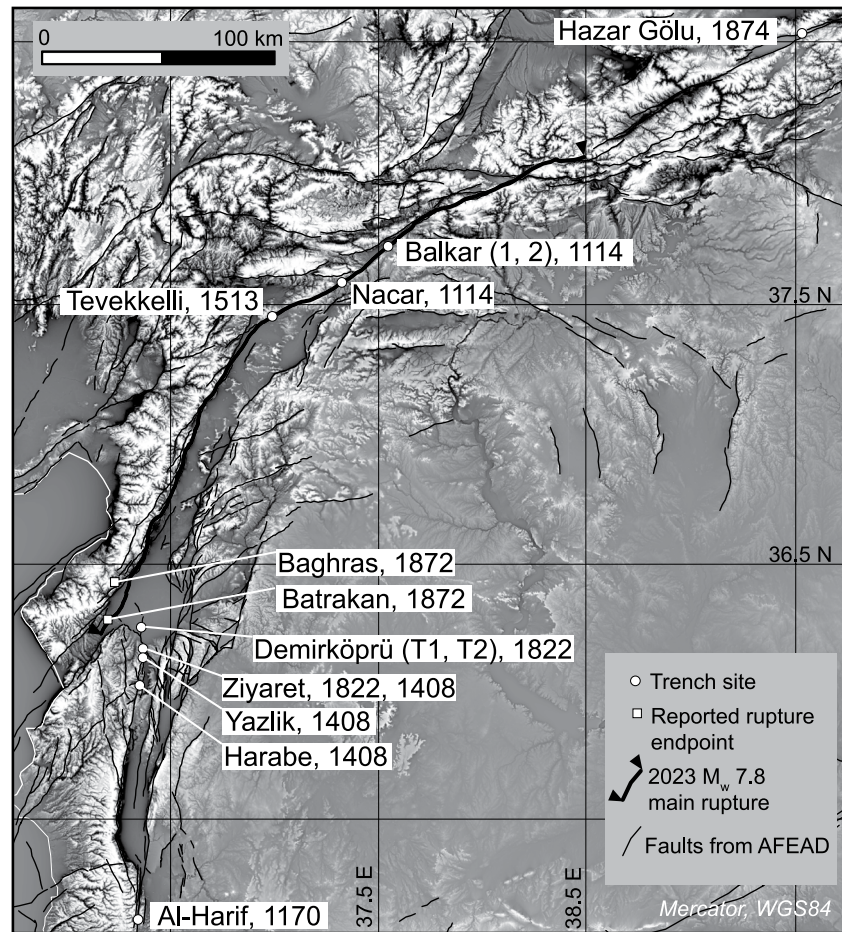


Figure 3. Location and names of trenches, and approximate historical fault rupture endpoints mentioned in the text, with the relevant pre-2023 earthquake/s indicated for each one. See references in text for each trench name. Active Faults of Eurasia Database (AFEAD) faults are from Zelenin et al. (2022), whereas the 2023 main rupture we remapped ourselves from the pixel tracking data of ForM[®]Ter—EOST (2023) and Ou et al. (2023), and from the preliminary maps of Reitman et al. (2023). Basemap derived from the 30 m GLO-30 Copernicus Digital Elevation Model (European Space Agency, 2021), processed by applying the texture shading technique of Brown (2014).

to be credible source faults for events of M_w 7 and above. We will start our analysis from those earthquakes for which there is the most information available, and which may appear in one or more of the trenches, then move to events which are less well-constrained. The order is not going to be strictly chronological, because some of the older events are well-constrained, and some of the more recent ones are not. We are going to start from the Amik basin area (Figure 1a), where the EAF and DSF come together, and move first south and then north. The final list of earthquake/fault pairs that we have determined to be the most likely can be found in Table 2, and the faults are shown in Figure 2b.

There are a few criteria that can be applied to the identification of the likely source fault of a historical earthquake in the absence of dating of geological or archeological features: (a) empirical relationships (e.g., Wells & Coppersmith, 1994) between earthquake size and fault parameters (a large earthquake must have a long rupture, so determination of epicenter position alone is not very meaningful), (b) the principle, based on Coulomb stress theory, that the same fault segment or neighboring parallel faults (i.e., side-by-side) with the same kinematics are highly unlikely to produce two large earthquakes within a few years or even decades of each other, and (c) careful reading of earthquake effect descriptions, paying particular attention to discussions by previous authors concerning reliability of sources. The latter is especially important because it is not uncommon for mistakes to be spread from one earthquake catalog to the next (or newly introduced) when information is accidentally left out, or two smaller earthquakes are conflated into a larger one.

A new source of information that we have today, which was not available when all the work on historical earthquakes in this region was being carried out, is the occurrence of the 2023 M_w 7.8 and 7.5 Turkey/Syria earthquakes (M_w from U.S. Geological Survey, 2023), which allowed us, for example, to verify that the empirical relationship used by previous authors to estimate magnitudes for historical earthquakes in this region is indeed appropriate (see Appendix A for details). This earthquake is also invaluable in that it shows how fault segmentation can be overcome to produce a very large earthquake, that is, we should not fall into the trap of automatically assuming a rupture cannot propagate past a bend or step when examining historical earthquakes.

All the earthquakes that we consider are between 1000 CE and 2023, so “CE” is mostly omitted throughout the paper. As no year has two earthquakes, throughout the text for simplicity we only refer to the year of occurrence, omitting day and month. The precise date of each earthquake (when known) is given in Table 2. Due to the fact that locality names and fault names are very much relevant in this kind of work, in addition to the maps in Figure 1 we have supplied details of naming (including rationale for specific choices) in Appendix B, and a full searchable list of locality names with alternates as Data Set S1. Finally, as the number of place names is quite large, we will not call a figure every time a place is mentioned: this paper should be read with Figures 1 and 2 at hand at all times.

2.1.1. Amik Basin and Dead Sea Fault Zone

We now apply the criteria described above to the earthquakes of 1872 and 1822. We start with this pair because the 1822 earthquake was singled out by Ambraseys (1989) not only as one of the largest earthquakes in the records, but also as one that took place in a region that—until February 2023—had very low seismicity.

Altunel et al. (2009) attributed the last event in their trenches at Demirköprü (Figure 3, dated to between 1801 and 1940) to the 1872 earthquake based on their interpretation of Ambraseys's (1989) paper: “Ambraseys (1989) reported that the 1822 earthquake took place in the Karasu Valley located further north of the Amik Basin [...] it is therefore unlikely that the event E1 can be related to the 1822 earthquake. Ambraseys (1989) also reports that the 1872 April 3 earthquake was responsible of heavy damage north and south of the former Amik Lake, and in particular [...] around Quillig and Armenez. On the basis of both paleoseismic results and historical accounts, we suggest that event E1 in trenches is related to the 1872 earthquake.” Ambraseys (1989), however, in the very next sentence to the one rephrased by Altunel et al. (2009) also states (concerning the Quillig area and the 1872 earthquake): “Here, it is said, the earthquake split the ground in places and yellow sand filled the area, a description suggesting widespread liquefaction.” Liquefaction can happen at large distances from a fault surface rupture (Ambraseys, 1988; Papathanassiou et al., 2005), so evidence of liquefaction is not evidence for surface rupture at or near liquefaction location. In 2023, the M_w 7.8 earthquake caused liquefaction in Kumlu (Quillig) and many other localities in the southern and eastern Amik basin, even though the fault rupture was along the Amanos mountains front, and liquefaction was reported also from localities up to at least 40 km away (Taftoglou et al., 2023). Furthermore, Ambraseys (1989) continues by writing, about the 1872 event: “Also, between Batrakan and Qaralu, the valley to the east of the hills is said to have dropped [...] and the ground was “rent” all the way to Baghras, an allusion to faulting.” The last three localities mentioned are at the foot of the Amanos mountains, about 20 km apart along the mountain front, and 18 km west of the trench site (Figures 1b and 3). Finally, the presumed location of the epicenter of the 1822 event has no bearing on whether the source fault can or cannot pass through the trench, because the epicenter of a historical earthquake simply indicates the center of the area of maximum damage (i.e., the center of the “epicentral region”), but the source fault of the 1822 event must be at least 100 km long based on magnitude/length relationships, so it could easily go through the trench site and have an epicenter elsewhere to the north. In fact, the isoseismals (lines of equal seismic intensity) plot for the 1822 event of Ambraseys (1989) shows the maximum intensity as an elongated region trending north-northeast, where the largest intensity isoseismal contains the trench location.

If we consider all the evidence together, the most logical interpretation is that the likely source of the 1872 event was the southernmost tip of the Amanos segment and, given the widespread damage also reported all the way from Antakya to Samandağ, and in the mountain villages on the Amanos mountains aligned parallel to this trend (Ambraseys, 1989), the faulting likely extended in that direction toward the coast, possibly by linking with faults in the Antakya fault zone (Figure 2b). Ambraseys (1989) plots isoseismals aligned with the southern termination of the Amanos segment and centered on the Hatay graben. Ambraseys and Jackson (1998) stand by the earlier interpretation of ground rupture for the 1872 event, as they report a 20 km rupture length for this event in their catalog of “surface rupturing earthquakes.” This leaves the 1822 earthquake as the only possible rupture in the

1801–1940 age range to go through the trenches at Demirköprü, because it is very unlikely that an unknown ground-rupturing earthquake (i.e., a large one) would be missing from the records after 1800, especially one that would have strongly affected such a historically important river crossing as the one at Demirköprü. If this is the case, then also the event of compatible age (“after 1650 CE”) found by Akyüz et al. (2006) in the next trench further south (Ziyaret, Figure 3) should be the 1822 earthquake.

The 1822 earthquake was a large event, as shown also by the fact that it was followed by 1.5 years of rather large aftershocks (Ambraseys, 1989, 2009), with the full aftershock sequence terminating only after 30 months (Salamon, 2008). Ambraseys (1989) and Ambraseys and Jackson (1998) estimated a magnitude of 7.5, which seems reasonable given the large area it affected and the level of damage reported everywhere. Without explaining why, Sbeinati et al. (2005), though also describing this as one of the most damaging earthquakes in the region, reduced the magnitude to 7.0. A clue to the magnitude change could be the fact that several localities in Turkey that had reported considerable damage (e.g., Gaziantep, and the towns west and northwest of it) are not listed in their catalog, which would reduce the size of the affected area and thus the magnitude. As there is no reason for the omission of these localities, we accept the determination of M_w 7.5 of Ambraseys and Jackson (1998).

Different authors have placed the 1822 event either on the Amanos fault (e.g., Seyrek et al., 2007), the Yesemek fault (e.g., Ambraseys & Melville, 1995; Duman & Emre, 2013), or the St. Simeon fault (e.g., Darawchek et al., 2022; Karakhanian et al., 2008). Even not considering the likely presence of this earthquake in the trenches of Altunel et al. (2009) and Akyüz et al. (2006) along the Orontes river valley, the Amanos fault is the least likely option: (a) the damage pattern from the 1822 M_w 7.5 earthquake is shifted east and south compared to the damage pattern of the 2023 M_w 7.8 earthquake (which definitely ruptured the Amanos segment, see Figure 2b), (b) several foreshocks (the strongest preceding the mainshock by 30 min) occurred in the region between Antakya, Latakia and Aleppo (Ambraseys, 1989, 2009), suggesting that the main shock may have been triggered by the rupture of one of the many north-south faults between the northern Ghab basin and the Amik basin, and (c) the epicenter estimated for the 1822 event by both Ambraseys (1989) and Sbeinati et al. (2005) is located ~20 km east of the Yesemek fault trace, albeit 60 km apart in latitude in either work (the location shift is also likely due to the exclusion of the Turkish area around Gaziantep from the 2005 catalog). In addition, Duman and Emre (2013) found no signs of a recent rupture along the Amanos fault in the Karasu valley, whereas they claim that the Yesemek fault appears to show a fresher morphology, at least in its northern segment (which is the one they checked in the field, on the Turkish side of the border). Ambraseys (1989) identified the maximum intensity isoseismal as approximately parallel to and slightly west of the Gaziantep-Kilis-Idlib trend. This is consistent with the position and orientation of both the Yesemek fault and the northern segment of the St. Simeon fault. Darawchek et al. (2022) explicitly argue for the 1822 event to have originated on the St. Simeon fault. These authors, however, identify as source fault what they call the “middle segment” of the St. Simeon fault (actually, it is the southern segment, see Figure 4): this is a mere 26 km long and a series of very short en-echelon segments (possibly a shear zone without a throughgoing fault near the surface), that is, too short to produce an earthquake of this magnitude. Considering the parameters quoted by these authors (M_w 7.3 and a fault width of 15 km), an average fault slip of about 10 m would be required, which is unrealistically large, as this is the typical average slip value for M_w 8.0 (Wells & Coppersmith, 1994). A 26 km long fault would normally produce roughly a M_w 6.7 earthquake, which does not match at all the historical descriptions of destruction spread over a vast region. For the St. Simeon fault to be the source of the 1822 earthquake, it would have had to rupture all the way from Afrin in the north to Sahen in the south (i.e., rupturing part of the Apamea fault as well), breaking across the southern segment too, which has a trend ~30° off from that of the two adjacent faults and, as pointed out above, appears to be more a broad shear zone than a throughgoing fault. Also, if a surface rupture had extended to the northeastern Ghab basin, the intensity at Maarret Missrin, Ram Hamdan, and Binnish (all between 6 and 12 km from the southern St. Simeon fault segment) should have been above the VII reported in Sbeinati et al. (2005). Finally, Karakhanian et al. (2008), while speculating that the 1822 event may have occurred on the northern segment of the St. Simeon fault (based on the epicenter location of Sbeinati et al., 2005), found no evidence of a recent surface rupture on it, including at the site of the St. Simeon monastery, which they studied extensively.

The most likely candidate for the 1822 earthquake thus appears to be the Yesemek fault combined with part of the Qanaya-Babatorun fault, with a rupture extending from the Yesemek fault northern segment for ~100–120 km south, past the Demirköprü bridge, to at least the Ziyaret trench of Akyüz et al. (2006) (Figures 2b and 3). The next trench south (Yazlık) does not have an event of compatible age, though it is possible that the event is simply not visible in the trench because it followed a slightly different strand. In any case, a rupture from the latitude of

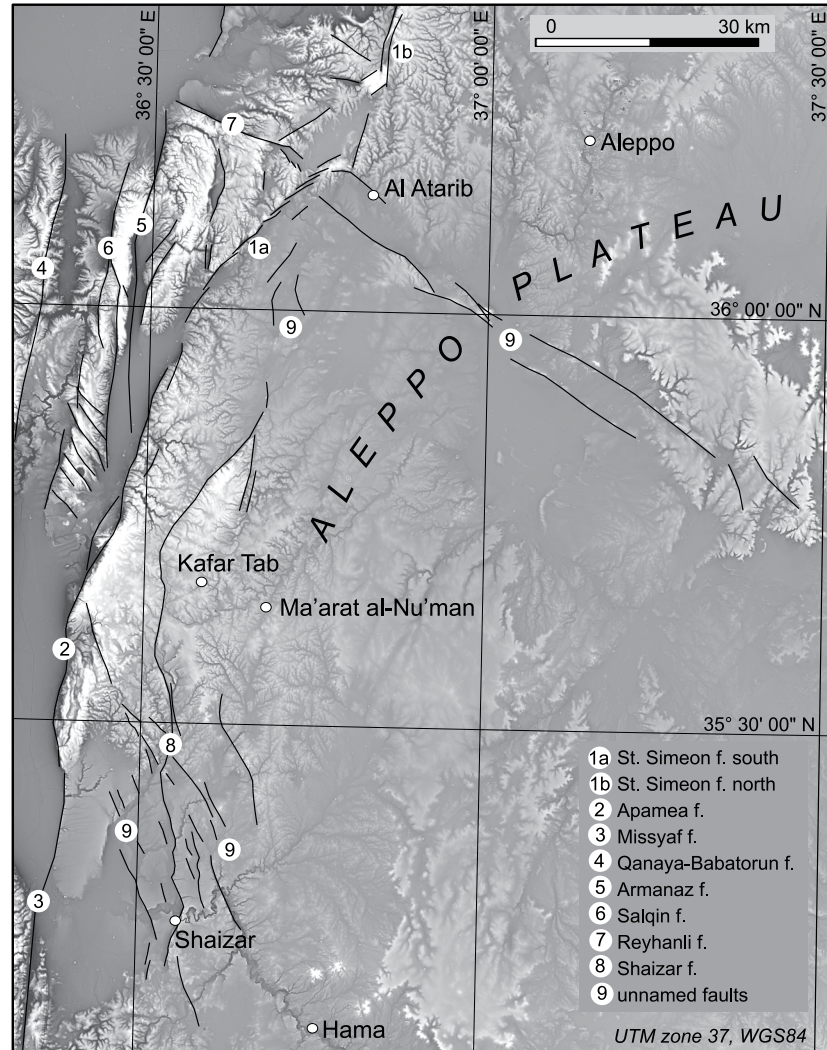


Figure 4. Faults that we mapped using the 30 m GLO-30 Copernicus Digital Elevation Model (European Space Agency, 2021) processed by applying the texture shading technique of Brown (2014), which can be used to enhance fine details (e.g., scarps). We mapped only the very sharpest features, which are likely to be active faults, but there are also numerous other more subtle lineaments. The background image has been muted for clarity; a full-strength and full resolution uninterpreted image is included as a Data Set S1.

Islahiye in the north to south past Demirköprü and into the Orontes valley would explain the especially strong damage in the Quseir region (which was also struck by numerous aftershocks, reported by Ambraseys, 2009) and at the main crossings on the Orontes river (Demirköprü and Jesr Al-Shughour), and the high damage region extending all the way to Sagce and Gaziantep in the north.

The Yesemek fault has usually been mapped continuing south to the eastern edge of the Amik basin (Duman & Emre, 2013) and possibly connecting to the Armanaz fault (Seyrek et al., 2014). The Yesemek fault, however, splits into two branches south of 36.616643°N, both of which are mapped as “active faults” in the active faults database of Zelenin et al. (2022). One branch (the one called “Yesemek fault” or “East Hatay fault” by previous authors, see Appendix B) continues with an almost N-S trend, whereas the other one turns southwest, following a series of low hills, then disappears under the sediments of the Amik basin (Figure 2). We also know that there is an active fault in the middle of the Amik basin. This fault is visible in the seismic line of Perinçek and Çemen (1990), and was re-interpreted by Seyrek et al. (2014), who reviewed and synthesized existing subsurface data. Old geographic maps also show that the eastern shoreline of the former Lake Amik and the eastern limit of the

swamps north of the lake followed this buried fault closely all the way to the eastern edge of the Karasu valley, meeting the Yesemek fault there. It seems likely that this is the source fault of the 1822 earthquake (Figure 2b), and that the fault interpreted by previous authors below the Amik basin is in fact the Yesemek fault, which continues south and connects to the Qanaya-Babatorun fault near Demirköprü.

The next pair of events that should be examined together is that of 1408 and 1404. The 1408 event has been identified most likely in all three trenches of Akyüz et al. (2006), who dated event E1 “between 1310 and 1423” in the northernmost trench and “younger than 1019” in the southernmost one. It could of course be either the 1404 or the 1408 earthquake, but as we will see the 1404 earthquake is unlikely to have ruptured this far north. The maximum destruction from the 1408 earthquake was along the trend from the Quseir region to Jesr Al-Shughour, with significant damage also to Mahalibeh castle, and damage to Jableh and Latakia along the coast. There is an open argument about the reported surface rupture, depending on the interpretation of the Arabic word for the distance, given as either ~20 km (Ambraseys, 1989, 2009) or ~2 km (Guidoboni & Comastri, 2005). The latter also claim there is no proof of damage in Antakya (which in their case means magnitude reduction from the 6–7 of Ambraseys & Jackson, 1998, to ~5.5), but Ambraseys (2009) reiterates that damage in Antakya is confirmed in reliable near-contemporary Ottoman calendar sources, which Guidoboni & Comastri (2005) do not seem to be aware of, as they do not mention them. Ambraseys (1989) puts forward two possibilities for the source fault: either the Qanaya-Babatorun fault, or the Antakya fault zone, the latter based on the fact that the damage extends toward the southwest to the coast. A matter of contention here is again the presumed surface rupture described in historical sources. Regardless of its length, the location of the rupture is debated, because there is no agreement on where the village mentioned in the ancient texts is located, near which the rupture may have terminated (the starting point was in the Quseir region, i.e., between Antakya and the Orontes gorge, so not very specific either). There are multiple spellings reported (Salthuam, Shalfuham, Salfhoum, Salthum), and this place is identified by Ambraseys (1989, 2009) as Hisn Tell Kashfahan (in Jesr Al-Shughour), and by Sbeinati et al. (2005) as Sfuhen (Sufuhon, on the eastern shoulder of the Ghab basin, Figure 1). The latter seems to be too far east, and located on faults that are not connected to anything in the Orontes gorge, but it could have been affected by a landslide triggered by the earthquake. So, if Sufuhon is indeed the location mentioned, a landslide and a fault surface rupture must have occurred at two different places. If Hisn Tell Kashfahan is the correct interpretation, then landslide and fault surface rupture could have been at the same place. Either way, the earthquake seems to have particularly affected one location that is clearly identifiable: the twin fortresses of Shugr and Bekas (Shugur Qadim), located less than 2 km west of the Qanaya-Babatorun fault. The key crossing on the Orontes of Jesr Al-Shughour, which sits on this fault trace, was also destroyed. In Antakya, however, the damage does not appear to have been as extensive, so the Qanaya-Babatorun fault seems a far more likely candidate than the Antakya fault zone, even without considering the information from the trenches. The fault rupture most likely did not extend north past the northernmost trench of Akyüz et al. (2006), because otherwise we would expect reports of destruction at the Demirköprü historical “iron bridge,” as this crossing was a vital one that had been in existence since well before 1000 CE. A ~40 km long rupture starting at about the northern trench site and extending to Jesr Al-Shughour would produce a M_w 7.0 earthquake, in line with Ambraseys and Jackson (1998) estimate of a “6–7” magnitude. A 20 km long rupture limited to the northern part of the fault appears too short to account for the significant damage extending all the way to Mahalibeh castle, and a 2 km long rupture is unrealistic, as the corresponding M_w 5.5 event would be too small to cause any damage along the coast in Latakia and Jableh, which are 70–80 km away.

There is less information for the 1404 earthquake: Ambraseys (2009) and Guidoboni & Comastri (2005) give essentially the same description from the same primary sources, and both point out that one source wrongly adds some 1408 localities to the 1404 event description. Sbeinati et al. (2005) used this source instead, apparently not realizing the problem, and estimated M_w 7.4. Ambraseys and Barazangi (1989) estimated $M_w \geq 7.0$. This means the surface rupture of the 1404 earthquake must have been at least 40 km long. From the damage distribution, the source fault has to be somewhere around the Ghab basin. The Qanaya-Babatorun fault is too far north to account for the significant damage to Marqab castle (on the coast, 25 km south of Jableh), and for the intensity VII–VIII reported from Tripoli in Lebanon. The Missyaf segment to the south is not a likely source, because the last event on this segment, visible in the trench and in the displaced Roman aqueduct at Al-Harif, is the 1170 earthquake (Meghraoui et al., 2003; Sbeinati et al., 2010). The two likely sources left are the Nusayriyah fault at the western margin of the Ghab basin, and the Apamea fault at its eastern margin (Figure 2a). We believe the Nusayriyah fault to be the more likely source, based on two considerations. The first is that the high damage

reports are skewed toward the coast, pointing to a source on the western rather than eastern Ghab basin, and the second is that an earthquake on this fault segment in 1404 would be more effective in increasing the stress on the Qanaya-Babatorun fault, which ruptured just 4 years later, than an earthquake on the Apamea fault. A final possibility, which we cannot discount at this time, is that the earthquake resulted from the rupture of a fault buried in the middle of the Ghab basin, as the presence of a fault here is known from geophysical data (Rukieh et al., 2005).

The next significant event back in time in this area is the 1170 earthquake, which is well-documented, with extensive descriptions by multiple authors (e.g., Ambraseys, 1989, 2004, 2009; Guidoboni, Bernardini, Comastri, & Boschi, 2004; Guidoboni & Comastri, 2005). Guidoboni, Bernardini, Comastri, and Boschi (2004) estimated M_w 7.7 ± 0.22 and a fault length of 125 km. Ambraseys (2009) instead estimated M_w 7.3 ± 0.3 . The source fault of this earthquakes has been identified by Meghraoui et al. (2003) as the Missyaf segment of the DSF, with the 1170 event being the last rupture that occurred at the Al-Harif aqueduct site. They suggested that the fault ruptured from Qalaat El Hosn to Apamea, a distance of ~ 80 km. Meghraoui et al. (2003) and Sbeinati et al. (2010) established that the slip at the aqueduct site in the 1170 event was 4–4.5 m. If this is maximum slip, it alone indicates M_w 7.3–7.4. This is compatible with the magnitude estimate of Ambraseys (2009), and reasonably compatible with the damage distribution. The only outlier is the city of Aleppo as reported by Guidoboni, Bernardini, Comastri, and Boschi (2004), but Sbeinati et al. (2010) argue that these authors overestimated the damage in Aleppo based on an erroneous interpretation of the chronicle by Ibn Al Athir. The argument of Sbeinati et al. (2010) is reasonable, because the damage distribution is otherwise very unusual, with a single intensity X locality (city of Aleppo) isolated and 200 km away from the main intensity X region (Lebanon-Syria border southwest of Qalaat El Hosn). We therefore agree with the source fault identification and rupture length of Meghraoui et al. (2003) and Sbeinati et al. (2010).

In 1156–1157 there was a long earthquake sequence (an “earthquake storm”) in the region between Homs and Aleppo, culminating with the largest event on 12 August 1157 (Ambraseys, 2004, 2009). Guidoboni, Bernardini, and Comastri (2004) did not calculate magnitude or epicentral area because of the difficulty in separating the numerous earthquakes in this period. Ambraseys (2004, 2009) instead separated several of the larger events and calculated the magnitude of the largest (7.2 ± 0.3), and placed the location of the epicenter very close to the Missyaf fault near Apamea. As mentioned above, the Missyaf fault last ruptured in 1170 through the Al-Harif site. While it is possible that an older rupture followed a slightly different strand and did not pass through the Al-Harif site, the Coulomb stress shadow due to an earthquake in 1157 would have most likely precluded another large rupture of the same fault segment just 13 years later, because such a short time is insufficient to significantly reduce the coseismic stress shadow from a $M_w > 7$ event. Based on the damage pattern, the St. Simeon fault is too far north, and the Nusayriyah fault too far west. That leaves the Apamea fault and another unnamed fault of similar length just 10 km east of it (which here we name “Shaizar fault,” Figures 2a and 4). Because it appears that the most damage was toward southeast (Hama, Salamiyah) and east (Ma'arat al-Nu'man, Kafar Tab, Shaizar) of the Ghab basin, the Shaizar fault is a more likely source than the Apamea fault. Sbeinati et al. (2005) put the epicenter on the Shaizar fault. Also, all of the 1156–1157 seismicity was concentrated in the region between Aleppo and Hama east of this fault. The area is littered with small faults (Figure 4), so it is conceivable that this is a case of small and moderate earthquakes triggering one another, until one of them got close enough to trigger the largest of these faults to rupture. The Apamea fault cannot, however, be excluded as a possible source without further investigation.

We have previously argued that the St. Simeon fault is unlikely to be the source of the 1822 earthquake. There are two older earthquakes, however, which could have been produced by this fault, in 1626 and 1138. The interpretation of this fault is controversial: some authors (e.g., Seyrek et al., 2014; Westaway, 2004) claim that it belongs to an earlier tectonic phase and it is no longer active. Others (Rukieh et al., 2005) instead consider it active, and some (Karakhanian et al., 2008) have even found evidence of historical earthquake-related deformation along it, albeit not an actual rupture of the main fault itself.

There is little information about the 1626 earthquake. Ambraseys only mentions it in his 2009 catalog and in Ambraseys and Finkel (1995), and Sbeinati et al. (2005) repeat the same information, add one paragraph, and estimate a magnitude of 7.3. It appears to have been a fairly damaging earthquake over a large area, but not much specific information has come to light. Karakhanian et al. (2008) consider the St. Simeon fault a likely source, based on their archeoseismological work on the St. Simeon monastery. A rupture of the northern segment of the

St. Simeon fault (~50 km long) could produce a M_w 7.2 earthquake, and in light of the reported damage area (between Aleppo and Gaziantep) we believe that this fault is indeed a likely candidate.

The authors who report extensively on the 1138 event are Ambraseys (2004, 2009), Guidoboni, Bernardini, and Comastri (2004), and Guidoboni & Comastri (2005). Sbeinati et al. (2005) just give it a brief mention, and this event does not even appear in the GEM historical catalog of Albini et al. (2013). An estimated magnitude is only reported by Guidoboni & Comastri (2005) (M_e 6.0), and apparently recalculated (without explanation, but from comparing the reported intensities it seems it was done by just increasing the estimated intensity values) in the INGV catalog to M_e 7.5 (Guidoboni et al., 2018, 2019). Both Ambraseys (2004, 2009) and Guidoboni & Comastri (2005) essentially give the same description concerning localities and damage, and date of the earthquake. Guidoboni & Comastri (2005) also calculate the position of the epicenter on Mount Quros, which is just 15 km north of the termination of the St. Simeon fault. On the basis of where the highest damage was, and where the earthquake was felt, the St. Simeon northern straight segment, which could produce a M_w 7.2 earthquake, is a likely source. The estimated M_e 7.5 (INGV) is excessive, because it corresponds to a 110–120 km long rupture, which would mean a rupture involving also the Apamea fault into the northern Ghab basin, with a very different damage distribution. In fact, Guidoboni, Bernardini, and Comastri (2004) suggested that the entire 1138–1139 sequence involved faults north-northeast of the Ghab basin, and not any of the faults that bound the basin itself. Besides the northern St. Simeon fault, there are no other long enough faults in the vicinity and in the proper position that would give the observed damage pattern. A magnitude of 6.0 (Guidoboni & Comastri, 2005) on the other hand is too small, because such an earthquake would have a radius with strong (VI) shaking of only about 20–30 km, and several localities that reported significant damage (e.g., Tell Khalid, Tell Amar, Bizaah) are 60–100 km away.

2.1.2. Karasu Valley and East Anatolian Fault Zone

The pairing of earthquakes and source faults along the EAF north of the Karasu valley, between Türkoğlü and Elâziğ, is somewhat more straightforward—albeit not entirely free of controversy—because there are fewer active faults that need to be considered, and fewer post-CE 1000 large earthquakes. We have included one earthquake from 2020 with M_w 6.8 (Elâziğ earthquake, Table 2), which is below our M_w 7.0 limit, because this is the only instrumental, twenty-first century and pre-2023 earthquake to have occurred along the EAF and it delimits the 2023 M_w 7.8 rupture northeastern extent (Figure 2b), so it is included here for completeness. This earthquake ruptured part of the Pütürge segment and did not appear to have a surface rupture (K. O. Çetin et al., 2020), though ~0.5 m of shallow slip was identified by Pousse-Beltran et al. (2020).

The 2020 Elâziğ earthquake rupture is sandwiched between two other relatively recent events: 1874 M_w 7.1 and 1893 M_w 7.2 ± 0.1 (Ambraseys, 1989, 2009; Ambraseys & Jackson, 1998). Ambraseys (2009) reported that he confirmed in the field in 1967 the surface rupture of the 1874 event, which involved the Palu segment between Palu and Pütürge (Ambraseys & Melville, 1995). His evaluation of the historical documents indicates a ground rupture about 45 km long, with 1–2 m uplift of the eastern block and unspecified left-lateral strike-slip displacement.

The 1893 calculated epicenter (Ambraseys, 2009) is near Çelikhan, and Ambraseys and Melville (1995) attributed the earthquake to the Erkenek segment. In the historical reports a surface rupture is not described anywhere, but for an earthquake of this magnitude it would be in the range of 45–70 km long. The rupture did not propagate south into the Pazarcık segment, as there is no trace of it in the Balkar and Tevekkelli trenches (Figure 3 of Yönlü (2012)). On the basis of the isoseismal plot and epicenter location of Ambraseys (2009), the earthquake likely ruptured most of the Erkenek segment, stopping ~20 km SW of Pütürge in the north, and near Erkenek in the south (Figure 2b). A smaller (M_w 6.8) event in 1905 with a similar epicentral area may have completed the rupture of this fault segment to the south, likely without a surface rupture (it does not appear in the “surface rupturing” event list of Ambraseys and Jackson (1998), whereas the 1893 event does).

The last rupture of the Pazarcık segment prior to 2023 is well-documented, because multiple trenches have been excavated across it (Yönlü, 2012). There are two historical large events in the vicinity of this segment that we need to consider: one in 1114, and the other in 1513/1514. The oldest of the two is the better documented one, even though it appears as two separate events in different catalogs. This earthquake is discussed in detail by Ambraseys (2004), who reported it as having happened on 29 November 1114. Ambraseys (2004, 2009) went to some length to explain why there are differences in reported dates, and concluded that 29 November

1114 is the correct one. This earthquake was assigned a magnitude of “large” (i.e., 7.0–7.8) by Ambraseys and Jackson (1998), and 6.9 ± 0.3 by Ambraseys (2009). Guidoboni & Comastri (2005) instead split the event in two, on different dates and locations (13 November 1114 Maraş, M_e 6.3, and 29 November 1115 Misis, M_e 6.4). Ambraseys (2009) states that it is unclear why they split the event and that in 1114 there were several other strong shocks in the region before the one on 29 November but the latter was by far the largest one in the series. One of the two shocks of Guidoboni & Comastri (2005) (13 November 1114) is in fact listed as a separate foreshock by Ambraseys (2009). Ambraseys (2009) also reported that some sources mention an earthquake in this region in 1115, and this was likely a strong aftershock. Sbeinati et al. (2005) also split the earthquake into two events that have same description and same general area, but different magnitudes (7.4 and 7.7), both of them in November 1114 (no day given, they just state within the same entry that this event could be two earthquakes). Here the confusion is increased by the fact that in the parametric list the authors supply two distinct epicenters and magnitudes, but an identical list of affected localities and intensities, so it is unclear how they were able to compute different epicenters and magnitudes. One of the two (M_w 7.4, with epicenter near Şanlıurfa, east of the Euphrates valley) has been included in the GEM catalog of Albini et al. (2013), whereas the second 1114 earthquake in the GEM catalog has been taken from Ambraseys (2009), again a choice without apparent explanation. There is no trace in Ambraseys's papers and in his 2009 catalog of any events in 1114 that affected mainly the region around Şanlıurfa: the two significant “foreshocks” mentioned were in the Iskenderun bay region. In fact even the 1115 event of Guidoboni & Comastri (2005) is located between the Iskenderun bay region and Maraş. Ambraseys (2009) stressed how the descriptions of this earthquake are split between “western” and “eastern” primary sources: this could explain the tendency of recent authors to produce two main shocks for the same event. Finally, the parametric catalog of Kondorskaya & Ulomov (1999) lists for this event M_w 8.1, and the event epicenter location (a single one for 1114, but on August 10, the date for which Ambraseys (2004) reports a strong shock possibly offshore Iskenderun) is placed between the locations of Ambraseys (2004) and Sbeinati et al. (2005). Considering that M_w 8.1 is close to the magnitude expected for a complete rupture of the entire EAF, this catalog clearly overestimates the size. In summary, for the earthquake of November 1114 the works of Ambraseys are more reliable, because there is a justification for each determination made (date, location, magnitude) and clear exclusion of other possibilities. We therefore chose to accept the information given in the latest work (Ambraseys, 2009) for the parameters of this earthquake, which place it somewhere along the Pazarçık segment of the EAF. Yönlü (2012) found a rupture compatible with a 1114 event in three trenches along the EAF (Nacar, and Balkar 1 and 2, Figure 3): there E1 has been dated to before 1153 and after 677, and this rupture is not present in their Tevekkelli trench, 35 km further southwest along the fault. From the paleoseismological findings a surface rupture length of 60 km has been estimated (Gürboğa, & Gökçe, 2019), placing the 1114 earthquake on the northern two-thirds of the Pazarçık segment with M_w of at least 7.1. This is compatible with the size estimated by Ambraseys (2009), but not with the estimates of Guidoboni & Comastri (2005), Kondorskaya & Ulomov (1999), and Sbeinati et al. (2005), further confirming that the earthquake location of Ambraseys (2009) is most likely the correct one. This event does not appear in any form in the trenches and core from Lake Hazar (Hazar Gölü, Figure 3; H. Çetin et al., 2003; Hubert-Ferrari et al., 2020), so probably its magnitude was not larger than the estimated 7.1, even though Ambraseys and Jackson (1998) considered it a possible candidate for a truly large earthquake (i.e., of magnitude closer to 7.8 than to 7.0).

The only authors to report on the 1513 earthquake in recent papers and catalogs are Ambraseys (1989, 2009), and Ambraseys and Finkel (1995). The exact year (late 1513 or early 1514) is also debatable. There is very little specific information about the earthquake, but Ambraseys (1989) claims that, given the size of the area over which it was felt (even in the absence of specific damage descriptions), the magnitude was significant (≥ 7.4). Apparently, the regions of Tarsus, Adana, Malatya, and around Haçin were strongly affected. His calculated epicenter location puts the earthquake within 30 km of the EAF (~ 30 km east-northeast of Türkoğlu), while the uncertainty radius is ~ 50 km, so a location of the event on the EAF is entirely plausible. The Tevekkelli trench of Yönlü (2012) contains a rupture for E1 dated to between 1440 and 1630, which is compatible with an earthquake in 1513/1514. In the three trenches further northeast along the EAF (Nacar, and Balkar 1 and 2) instead E1 is dated to between 677 and 1153, so the 1513 event is not visible. The closest trench to Tevekkelli (the Nacar trench) is 35 km northeast of it, so the rupture should have stopped before reaching this point, which means it is unlikely for the 1513 earthquake to be the penultimate event (E2) tentatively identified by H. Çetin et al. (2003) in one of their Lake Hazar trenches (they date E2 to 1393–1464 CE, but claim that, because of dating uncertainties, it could be the 1513 earthquake). In the catalog of trenches in Turkey (Gürboğa & Gökçe, 2019), the 1513 rupture is estimated as 40 km long. This is barely the equivalent of a rupture of the Pazarçık segment between about

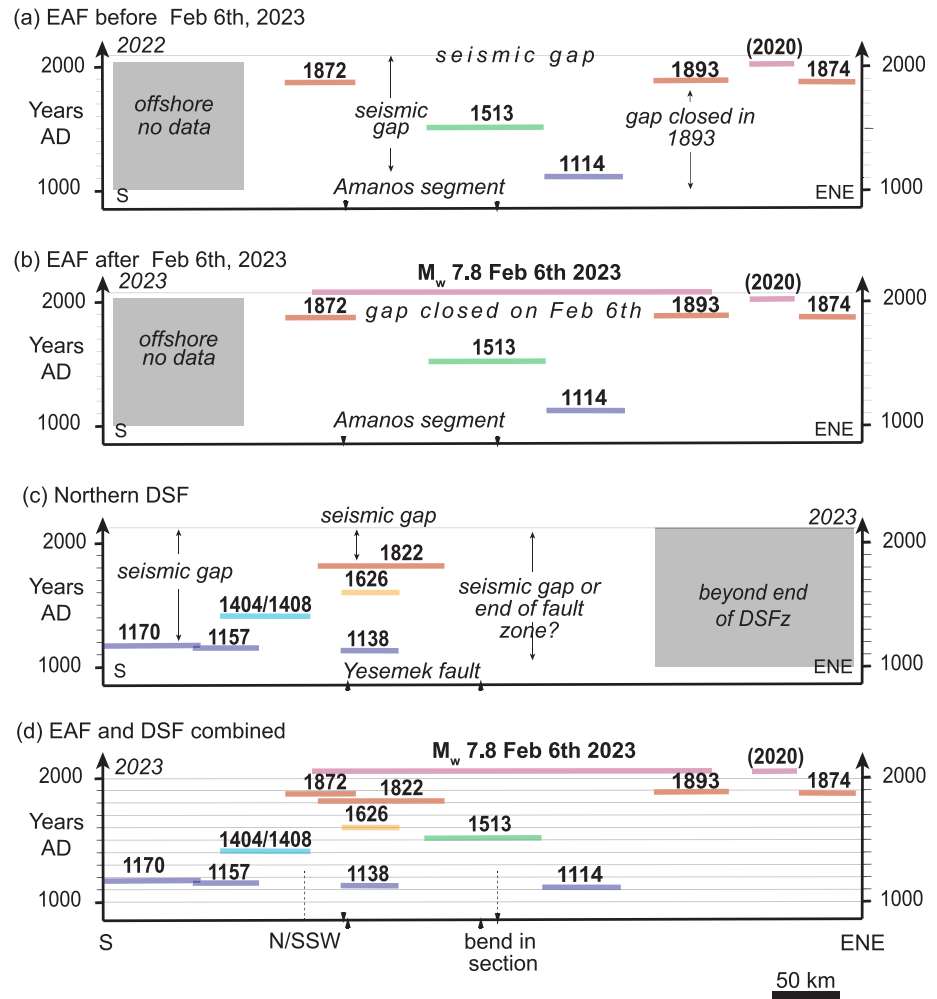


Figure 5. Space-time pattern of historic earthquakes along the East Anatolian Fault (EAF) and northern Dead Sea Fault zone (DSF) (see Figure 2 for location). The position and extent of $M > 7$ ruptures (horizontal bars) are justified in the text. (a, b) Pattern of $M > 7$ ruptures for the western portion of the EAF prior to and after 6 February 2023. (c) Pattern of $M > 7$ ruptures for the northern DSF. (d) Pattern of all recorded $M > 7$ ruptures for the region in which both active strike-slip fault systems (EAF and DSF) overlap spatially and interact kinematically.

10 km southwest of the Nacar trench and Türkoğlu. A 40 km rupture however would not produce an earthquake above M_w 7.0. A M_w 7.4 earthquake requires a 80 km long rupture. That can be done by the rupture extending from south of the Nacar trench to Islahiye, that is, rupturing the southern part of the Pazarcık segment and then the Nurdağı segment of the Amanos fault to the next bend south near Islahiye (Figure 2b). This would be more in line with an event that must have produced considerable damage to the region of Adana and Tarsus. A rupture stopping at Türkoğlu and a M_w of 7 would not have been sufficient, this region being 180 km away.

3. Discussion: Timing, Location, and Size of the 2023 M_w 7.8 Pazarcık Earthquake

3.1. Fault Segmentation, Rupture Length, and Earthquake Size

In the Karasu valley, the central and southern Amanos fault (Hassa segment and most of the Kirikhan segment, Figure 2a) does not appear to have ruptured in a large earthquake at any time from at least 1000 CE to 2023 between Baghras and Islahiye, a fault length of ~ 70 km (Figures 2b and 5a). This could partly explain the unusually large size of the 2023 M_w 7.8 earthquake: the central and southern Amanos segments, which are

separated from the Nurdađı segment by a releasing bend near Islahiye, and from each other by a restraining bend near Demrek (Duman & Emre, 2013), were stressed enough that the bends not only were insufficient to stop a multi-segment rupture but may have contributed to it. In fact, it appears that the Demrek restraining bend was a region of higher slip from the surface to ~10 km depth (Barbot et al., 2023). Recent studies on large thrust earthquakes (e.g., 2008 M_w 7.9 Wenchuan earthquake, Wan et al., 2017) suggest that stepovers along faults, and especially restraining stepovers, build up slip deficit over time merely because of their geometric complexity, and when they finally rupture they provide energy for the rupture to propagate even further, which it seems is what happened on the Amanos fault. Thus, the most likely reason we have not seen such large ruptures before on the EAF is not because “fault segmentation” or “fault maturity” determine the maximum length of rupture in plate boundary faults, but rather because they are infrequent and, therefore, not captured by the comparatively short and incomplete earthquake history we have for the region. For a M_w 7.8 earthquake to happen, which, let’s not forget, ruptured over half of the EAF at once, we need a rather specific set of circumstances that are hard to quantify in the absence of data.

Prior to 2023, there was considerable disagreement over the maximum size of earthquakes on the EAF. For example, Hubert-Ferrari et al. (2020), on the basis of the historical seismicity reports, assumed that magnitude 7.0 and above is likely, whereas some studies based on the instrumental record alone considered M_{\max} for the EAF to be limited to M_w 6.8 (e.g., Bayrak et al., 2015), while yet others proposed a range from M_w 6.7–7.4 depending on the segment considered (e.g., Gülerce et al., 2017; Güvercin et al., 2022), with up to M_w 7.7 when some segment combinations are explored in models (Gülerce et al., 2017). A good estimate of M_{\max} , however, is crucial for seismic hazard assessments. In the case of faults like the EAF, which have no large instrumentally-recorded events, knowledge about M_{\max} , recurrence intervals, and rupture length can only come from a combination of historical records, paleoseismological studies, geological analysis in tectonic context, and comparisons with similar faults. Based on the information available at the time, the 2023 M_w 7.8 earthquake could have been foreseen in terms of location and timing (an earthquake on the southern EAF was due any time, this fault being a clearly active one currently in—what should have been an alarmingly—quiescent period), but not in size, because the largest confirmed earthquake in historical catalogs since 1000 CE for the region reached M_w 7.5 at most, with the majority of earthquakes being M_w 7–7.2 (Table 2). Besides, the source fault of the M_w 7.5 earthquake in 1822 is not technically even part of the EAF system. Looking further back in time (before 1000 CE) would not have increased the number of truly large earthquakes, as such events are even harder to interpret the older the records are: there are none listed for this area by Ambraseys and Jackson (1998), but that does not mean none happened, just that they may not have been recognized or recorded. With no earthquakes of comparable size in either instrumental or historic catalogs, we cannot calculate an observed recurrence interval for $M_w \geq 7.8$ on the EAF, and are left with estimates based on geodetic rates or longer-term average geological displacement rates (e.g., Friedrich et al., 2003). This is only half the problem though: without a $M_w \geq 7.8$ in the records, the possibility that such an earthquake would occur on the EAF was not seriously considered in seismic hazard calculations for the region by most authors. We propose that for the EAF M_{\max} is actually ~8.2, that is, a complete rupture from the Karlıova triple junction to the Amik triple junction (Figure 1d), and that all continental strike-slip plate boundary faults should be treated as having the same end-to-end rupture potential, unless proven otherwise. In this context, M_{\max} is reached in “superevents” that are infrequent and most likely highly non-periodic, especially for non-isolated plate boundary faults such as the EAF-DSF system (contrast with the Alpine Fault, NZ, Berryman et al., 2012) and thus not captured by even such a comparatively long historical record as we have for Anatolia. The 2023 M_w 7.8 earthquake did not reach M_{\max} only by a fortuitous combination of circumstances. It appears that the combined effect of the larger stepover between the Erkenek and Pütürge segments and the coseismic Coulomb stress shadow from the 2020 Elâziğ event on the latter was enough to stop the 2023 rupture from dynamically propagating further to the northeast. Understanding how and in what measure fault geometry and prior stress history each contributed to stopping the rupture will need careful modeling. The 2023 M_w 7.8 earthquake stands as a warning that continental transforms can fully rupture just as subduction thrusts can (see McCaffrey, 2008), in infrequent but devastating earthquakes.

3.2. Fault Interactions, Cascades, Cycles, Supercycles, and Collective Memory

The reason for the behavior of the EAF is multifaceted. First of all, there is the intertwined kinematics of the three plate boundary fault systems: EAF, DSF, and NAF (Figure 1d). Hubert-Ferrari et al. (2003) pointed out that the EAF and NAF cannot move simultaneously, and that in the historical records since 100 CE the number

of damaging earthquakes on each fault reflects this, with peak seismic activity switching from one fault zone to the other every few hundred years. For the DSF, Khair et al. (2000) also observe a switching between activity and quiescence, with quiescent periods of 450–700 years interrupted by active periods of 50–150 years in the past two millennia. These are examples of supercycles (e.g., Philibosian and Meltzner, 2020; Salditch et al., 2020).

Whereas plate-boundary-scale kinematics and variations in long-term strain accumulation may control the acceleration and the turning-on-and-off of each fault zone on the million-year to the millennial scale (i.e., supercycles and clusters; see also Bennett et al., 2004; Friedrich et al., 2003; Lefevre et al., 2018), within each period of high activity the seismic behavior is likely controlled by coseismic and postseismic Coulomb stress changes (King et al., 1994). The latter is indicated by the clustering of earthquakes within relatively short time periods, and by the propagation of ruptures in systematic fashion along some faults: for example, the classic NAF behavior of east-to-west sequential ruptures (e.g., Barka, 1996; Hubert-Ferrari et al., 2000, 2003; Stein et al., 1997), but also the behavior observed on the EAF, where a series of ruptures can start at both ends of the fault system and move toward the center (Hubert-Ferrari et al., 2003). Another potential example of this behavior is the rupture cascade (Philibosian and Meltzner, 2020) of the twelfth century (cf. Figure 7.2 in Marco and Klinger, 2014) along the EAF and DSF systems in a southerly direction. The 1114 event occurred along the Parzarcık segment of the EAF (Figure 2b). Then, the DSF ruptured several times as documented by the 1138, 1157, and 1170 events (Figures 2b and 5), and the 1202 event in Lebanon (South Yammouneh segment, DSF, Daëron et al., 2007). After the twelfth century cascade, both fault zones appear to have ruptured irregularly. As a result, the time since the last major ($M_w > 7$) event varies along strike of the fault zones. For the EAF, the times since the last rupture events are 130 years (Erkenek segment), 500, 900, and over 1,000 years for the Amanos segment (Figure 5a). These seismic gaps are not due to a lack of data, but rather are an expression of the natural earthquake behavior in active fault zones. Thus, for fault segments where a seismic gap exists, the maximum possible earthquake magnitude (M_{max}) may be severely underestimated unless seismic activity from the entire fault system going back several thousand years is considered. For example, seismic hazard modeling conducted solely based on instrumental seismic records prior to 6 February 2023, treated such segments as inactive and underestimated M_{max} and the seismic hazard (e.g., Bayrak et al., 2015). The 6 February 2023 Pazarıcık earthquake filled in the large seismic gaps in the Amanos segment and several other seismic gaps along strike (Figure 5b). If the same type of hazard modeling would be conducted after 6 February the Amanos segment will appear as active and be included, thereby likely overestimating its hazards in the near future.

Similar seismic gaps also exist along the DSF, some lasting for 200 years, while others last for 620 years, and over 850 years (Figure 5c). These seismic gaps will grow, close, and reopen repeatedly (Figure 5d) as long as strain accumulates across this active plate boundary, and when a seismic gap exists without a recent stress shadow, the hazard is high. The identification of seismically inactive but geotectonically active regions along active fault zones is, therefore, an important area of focus for future research and seismic hazard assessment, but additional information is required to accurately forecast earthquake potential.

There is also an important role played by local fault configuration, in this case especially the branching of EAF and DSF. The two systems are not independent, even on short time scales. These two fault zones overlap, with faults from both zones running parallel to one another and having very similar kinematics in a strip just a few tens of km wide. Thus, in the Karasu valley and Amik basin, depending on exactly which fault ruptures where, there can be either Coulomb stress loading or shadowing of neighboring faults belonging to either fault zone. For example, the northwestern DSF strands (Qanaya-Babatorun and Nusayriyah faults) have likely been loaded coseismically by the 2023 M_w 7.8 earthquake, simply on the basis of their relative position, geometry, and kinematics. On the other hand, the Amanos segment and the Yesemek fault in the Karasu valley have the same configuration as the southern San Andreas/San Jacinto fault pair in California: two closely-spaced (15–30 km) subparallel faults with the same strike-slip kinematics. This is a situation where the faults are effectively coupled: a large rupture on one fault would cause a significant coseismic Coulomb stress drop on the other, delaying the next rupture (Carena et al., 2004). The 1822 earthquake on the Yesemek fault therefore must have delayed the occurrence of the next earthquake on the central-southern Amanos fault, which at that point had not seen a rupture for at least 800 years, and the end of this delay just happened to coincide with a fortuitous rupture propagation from a minor fault in the Narlı fault zone (Figure 2a) to the main branch of the EAF (Rosakis et al., 2023; U.S. Geological Survey, 2023), at a position on the Pazarıcık segment of the EAF that also had not seen a rupture in 900 years. This was a classic “domino effect” with all tiles in the right place at the right time. We are thus left with a question that can be answered only with further investigations: how often can the tiles

line up in this specific order? It is not a trivial problem: not only a specific set of circumstances can lead to an unusually large event, but also activity on one fault system could control the timing of the next supercycle of its immediate neighbor. It means that calculation of earthquake probability cannot be restricted to one fault, or even one fault system: in the case of continental plate boundary faults, it also needs to include the neighboring fault systems. Plate boundary faults may not just have a “long term memory” (Salditch et al., 2020), but also a “collective memory” due to their coupling by geometric characteristics of the fault systems and stress transfer patterns between them, which would call for earthquake probability calculation at much larger scales than is generally considered.

4. Conclusions

Within the limitations of the information available, we were able to define the most likely pairs of historical earthquakes and their source fault segments along the EAF and northern DSF since 1000 CE. We tried to provide a comprehensive explanation for the choices we made in each case, so that the data we produced can be evaluated for level of uncertainty, and used by others either for earthquake modeling, or to identify locations that should be targeted in future paleoseismological studies.

By considering the previous rupture history and geometric configuration of the faults involved, we were able to address the reasons why the 2023 M_w 7.8 earthquake occurred on the southern half of the EAF, why the conditions were right for it to occur now, and why it was unusually large compared to previous events in the region. The main branch of the EAF had a seismic gap of at least 1,000 years at its southern end. A major rupture here was likely delayed by the 1822 earthquake on the Yesemek fault (which could explain why the 1872 rupture did not propagate northwards), but the stress shadow from this dissipated in about a century, paving the way for any rupture to either initiate on or propagate unimpeded into the southern Amanos segment. Based on the historical seismic records of the region, the 2023 M_w 7.8 Pazarcık earthquake was foreseeable in space and time, but not in size. M_{\max} for the EAF is likely ~ 8.2 , with the limit rupture length being the distance between the two triple junctions that delimit it. The 2023 earthquake may not have reached M_{\max} simply by a fortuitous combination of factors: if the 2020 Elâziğ earthquake had not happened where and when it did, would the 2023 rupture have continued propagating toward the northeast? This is a question that could be answered by combining Coulomb stress models and dynamic rupture models. If nothing else, what we have learned from the 2023 M_w 7.8 Pazarcık earthquake is that segmentation of continental transform faults is not relevant for calculating M_{\max} , because some earthquakes can jump across segment boundaries. Such earthquakes are so infrequent, however, that they are difficult to study, and therefore hard to foresee.

Appendix A: Earthquake Magnitudes

For earthquake magnitudes between 6.2 and 8.2 and depth of focus <70 km, $M_w = M_s$ (Scordilis, 2006). As we only consider events in this magnitude range and discuss a few instrumental events for which M_w is reported, we always use M_w in our text unless it is necessary to specifically mention another type of magnitude, with the understanding that, when citing historical sources, these mostly reported either M_s determined using local empirical relationships based on rupture length, or M_F (“felt magnitude” equivalent to M_s , see below) (e.g., Ambraseys, 1988; Ambraseys & Barazangi, 1989). Another magnitude used by the INGV CIFT5Med catalog (Guidoboni et al., 2018, 2019) is M_e , which here stands for “magnitude equivalent” (i.e., equivalent to M_w) as calculated from intensities (whereas usually M_e stands for “energy magnitude” calculated from energy release) which, as far as uncertainties are concerned, we treat as M_F , because it is also fundamentally based on reported intensity areas. The difference between M_e and M_F appears to be simply the specific relationship between intensity and magnitude used, which for M_e is the one of Gasperini and Ferrari (2000). Considering that the largest source of uncertainty in estimating magnitude is the interpretation of the historical descriptions themselves, which determine what intensity is assigned to each place (e.g., where one author assigns intensity X, another may assign intensity VIII), the specific relationship used does not seem to be overly important, as long as it is properly calibrated for local conditions.

To better understand this source of uncertainty, we have recalculated magnitudes ourselves for all the historical earthquakes that we considered whenever sufficient information was available, using the M_F relationship developed for Turkey by Ambraseys and Finkel (1987) and re-interpreting assigned intensities from descriptions, if

necessary (especially in cases of conflicting opinions), before deciding which reported magnitude to adopt in our work:

$$M_F = -0.53 + 0.58(I_i) + 1.96 \times 10^{-3}(R_i) + 1.83 \log(R_i),$$

where R_i is the average radius (in km) of the isoseismal of intensity I_i .

The reason we used M_F in our own tests instead of M_s is because not all events have a reported rupture length (which, even when reported, may be underestimated, as discussed by Ambraseys & Jackson, 1998), but nearly all have at least a “felt area.” From comparing previous authors' works in this region with our own test results, the uncertainty in magnitude estimated for historical earthquakes of ± 0.3 (Ambraseys, 1989) seems to be about right (Table A1).

Table A1
List of Earthquakes With M_F Recalculated by Us, and All Magnitudes Reported by Previous Authors^a

| Date ^b | M_F | Reported magnitude ^a | Name ^b |
|-------------------|------------------|--|-----------------------|
| 6 February 2023 | 7.3 ± 0.2 | M_w 7.5, 7.6, 7.7 | Elbistan |
| 6 February 2023 | $7.7 + 0.2/-0.1$ | M_w 7.7, 7.8, 8.0 | Pazarcık |
| 24 January 2020 | 6.6 | M_w 6.7, 6.8 | Elâziğ |
| 2 March 1893 | 7.0 | ≥ 7.1 ; 7.2 ± 0.1 | Malatya |
| 14 January 1874 | 7.0 ± 0.1 | ≥ 7.1 | Sarikamiş |
| 3 April 1872 | $7.1 + 0.2/-0.1$ | 5.9 ^c ; ≤ 7.2 ; 7.2 | Amik Gölü |
| 13 August 1822 | $7.5 + 0.3/-0.2$ | 7.0; ≥ 7.4 ; 7.5 | Southeastern Anatolia |
| 21 January 1626 | – | 7.2 | Hama |
| 1513/1514 | $\geq 7.4^d$ | ≥ 7.4 | Malatya |
| 29 December 1408 | 7.1 ± 0.1 | 7.0; 6–7; 7.4 | Shugr-Bekas |
| 20 February 1404 | 7.4 | ≥ 7.0 ; 7.4 | Aleppo |
| 29 June 1170 | $7.3 + 0.2/-0.4$ | 7.3–7.4; 7.3 ± 0.3 ; 7–7.8; 7.7 | Shaizar |
| 12 August 1157 | 7.4 ± 0.1 | 7.2 ± 0.3 ; 7.4 | Apamea |
| 11 October 1138 | 7.1 ± 0.5 | 6.0; 7.5 | Atharib |
| 29 November 1114 | 7.3 ± 0.4 | 6.9 ± 0.3 ; ≥ 7.2 ; 7.4; ≥ 7.8 | Antioch, Maraş |

^aUnless M_w is explicitly indicated, the reported magnitude is either M_s , M_F , or M_c as explained in the text. ^bAmbraseys (2009) except for 2020 (K. O. Çetin et al., 2020) and 2023 events (U.S. Geological Survey, 2023). ^cSbeinati et al. (2005). It is unclear where they get this low value from, because it is very different from those of the authors they cite, and it seems to conflict with the size of the high damage area and the highest reported intensity when compared to the other events they have in the same catalog. ^dDue to the limited information, only one intensity area can be defined, so the magnitude depends on whether this intensity is assigned as VI or VII (because significant “destruction” was reported in all localities mentioned, it should be at least VI, i.e., strong shaking).

The addition of the 2023 events allowed us also to verify that this empirical relationship is indeed appropriate for the region, as the M_F we calculated for the two events using intensity maps from U.S. Geological Survey (2023) are $7.7 + 0.2/-0.1$ and 7.3 ± 0.2 respectively (Table A1). Considering that different seismological laboratories in the US and Turkey (USGS, GCMT, GEOSCOPE, KOERI) have variably reported M_w of 7.7, 7.8, and 8.0 for the first event, and 7.5, 7.6, and 7.7 for the second, our estimate of M_F is well within range and validates the use of this formula for older earthquakes in the region, with ± 0.3 also a reasonable, conservative uncertainty.

Appendix B: Fault Names and Place Names

There seems to be no generally accepted standard about names of faults and fault segments in the region. One problem is the political border between Turkey and Syria: as it happens too often, faults (and their names) have a tendency to end or change at the border. The Active Faults of Eurasia Database of Zelenin et al. (2022) often does not label the individual fault segments beyond naming the general fault zone to which they belong. For

the EAF system, we have decided to use the segment names and segment boundaries as defined in Duman and Emre (2013), because these authors go through the effort of systematically providing detailed maps, coordinates, and names in a way that is easy to follow. In the case of faults that are traditionally considered part of the Dead Sea fault system, the choice is less straightforward, because even when a fault has been labeled, its endpoints are usually ill-defined, or a vague description (e.g., “fault on the eastern side of the Ghab basin”) is given, and maps in publications are small and hard to read. We chose to use the labeling of Westaway (2004) and Seyrek et al. (2014) for the following faults: Qanaya-Babatorun (called instead “Hacıpaşa segment” to the Syrian border by Akyüz et al., 2006), Nusayriyah, Apamea, Salqin, and Armanaz, which are named after nearby towns and villages. These authors also define a “East Hatay fault” on the eastern edge of the Karasu graben, whereas the same fault is called “Yesemek fault” by Duman and Emre (2013). We chose to keep the latter name because it has been assigned based on the fault going through the village of Yesemek, whereas “East Hatay” refers to a region. Finally, different authors assign the name “Afrin” (or Aafrin) fault to two entirely different faults that pass near the town of Afrin. One of these two does not appear in our analysis, but to avoid any confusion, we have decided to call the fault that we discuss “St. Simeon fault” as named by Rukieh et al. (2005) and Karakhanian et al. (2008) due to the fault passing through the St. Simeon monastery site (whereas Westaway, 2004, and Seyrek et al. (2014), call this “Afrin fault”). We were not able to find any existing names for the faults east of Apamea in Syria (on the Aleppo plateau, between the Ghab basin and Aleppo, see Figure 4), so to avoid using the “unnamed” label more than necessary, we named the largest of these “Shaizar fault,” because it goes through the town bearing this name, which was destroyed in the 1157 earthquake.

Place names in this region have changed throughout the centuries depending on who controlled which territory, and even today the same name is spelled differently depending on transliteration and on native language of the writer. In reading the various publications and earthquake catalogs we had to go to some lengths to match place names from one publication to the next, and to modern-day names that anyone can find on Google Earth. Thus, besides the standard map with locations (Figure 1), we are also including a simplified table of place names in this appendix (Table B1), plus an electronic version of it that reports all the variants we have encountered (up to six), coordinates, and any comments where needed (Data Set S1). The list is by no means exhaustive, but it should help readers find their way from one publication to the next. In our paper we have decided which name to use mostly based on the primary source of our information, except for those cases where a modern name was easier to find in online searches and the name appears many times in our text (e.g., Demirköprü instead of Jisr al-Hadid). In those cases where the modern locality name has nothing to do with the one in historical records (we just matched positions between the published map and Google Earth map to identify its coordinates), we have kept the historical name in our text and maps, but supplied the name of today's nearest locality in the table (e.g., Batrakan/Atatürk).

Table B1
Place Names From Figure 1, Listed Alphabetically in First Column: In Bold Is the Version Used in Text and Figures

| Google Earth name | Alternate name 1 | Alternate name 2 |
|-------------------|--------------------|------------------|
| Afamiyah | Apamea | Afamea |
| Afrin | Aafrine | Aafrin |
| Al Atarib | Al-Atareb | Cerepum |
| Alazi | Qaralu | |
| Aleppo | Halab | Halep |
| Antakya | Antioch | Hatay |
| Armanaz | Armenhaz | |
| Asmacık | Tell Khalid | Trihalet |
| Atatürk | Batrakan | |
| Bakras Kalesi | Baghras | Bagras |
| Biza'ah | Bizza | |
| Demirköprü | Jisr al-Hadid | Jisr El Hadid |
| Gaziantep | Aintab | Gaziaintab |
| Hama | Hamat | Hamath |

Table B1
Continued

| Google Earth name | Alternate name 1 | Alternate name 2 |
|--------------------------|-------------------------------------|------------------|
| Haram | Harim | Uringa |
| Homs | Hims | Emesa |
| Iskenderun | Alexandretta | Scanderoon |
| Jableh | Jeble | Jabala |
| Jesr Al-Shughour | Jisr al-Shughur | Jisr as-Shugr |
| karamurt Hani | Qaramut | |
| Khan Shaykhun | Han Sheikhun | |
| Kharamanmaraş | Maraş | Germanicea |
| Kozkalesi | Quseyr | Quseir |
| Kumlu | Qillig | Quilliq |
| Latakia | Al-Ladhiqiya | Laodicea |
| Ma'arat al-Nu'man | Marre | Arra |
| Ma'arrat Misrin | Ma'aret Masrin | Megaret Basrin |
| Mahalibeh castle | Qalaat Blatnes | Balatunus |
| Marqab castle | Markab | Margat |
| Missyaf | Masyaf | Misyaf |
| Mount Kiliç | Mount Cassius | Al-Akraa |
| Orontes/Asi | Arantu | |
| Qalaat El Hosn | Krak (Crak, or Crac) des Chevaliers | Hisn al-Akrad |
| Saimbeyli | Haçin | Kaza Haçin |
| Sakcagoz | Sagce | Sakçagözü |
| Salamiyah | Salamiyya | Salamiyyah |
| Salqin | Salqein | |
| Samandag | Suaidiya | Seleucia |
| Şanlıurfa | Urfa | Edessa |
| Serjilla | Kafar Tab | Capharda |
| Shaizar | Shayzar | |
| Shugur Qadim | Castles of Shughur and Bekas | Shugr-Bekas |
| Tell Arn | Tell Harran | Tal 'Aran |
| Tilbasar Kalesi | Tell Bashir | Turbessel |
| Tripoli | Tarabulus | |
| Yakapınar | Misis | Mopsuestia |

Note. Full version in Data Set [S1](#).

Data Availability Statement

All the data and software we used have been published or made available by the authors and entities cited in the references list: digital elevation models (European Space Agency, 2021, <https://doi.org/10.5270/ESA-c5d3d65> [Dataset]; Tozer et al., 2019, <https://doi.org/10.1029/2019EA000658> [Dataset]), active fault database (Zelenin et al., 2022, <https://doi.org/10.5194/essd-14-4489-2022> [Dataset]), pixel-tracking data (ForM@Ter—EOST, 2023, [doi:10.25577/EWT8-KY06](https://doi.org/10.25577/EWT8-KY06) [Dataset]; Ou et al., 2023, <https://dx.doi.org/10.5285/df93e92a3adc46b9a5c4bd3a547cd242> [Dataset]), preliminary surface rupture mapping (Reitman et al., 2023, <https://doi.org/10.5066/P985I7U2> [Dataset]), and texture-shading program (Brown, 2014, <https://app.box.com/v/textureshading> [Software]). The file with the electronic version of the ruptures listed in Table 2 and shown in

Figure 2b is part of Supporting Information S1. We have also included in the supplement the uninterpreted base images of Figures 2b and 4.

Acknowledgments

We are grateful to Z. Cakir, J. Hubbard, and two other anonymous reviewers for their insightful comments. Open Access funding enabled and organized by Projekt DEAL.

References

- Akyüz, H. S., Altunel, E., Karabacak, V., & Yalçiner, Ç. (2006). Historical earthquake activity of the northern part of the Dead Sea fault zone, southern Turkey. *Tectonophysics*, 426(1–2), 281–293. <https://doi.org/10.1016/j.tecto.2006.08.005>
- Albini, P., Musson, R. M. W., Gomez Capera, A. A., Locati, M., Rovida, A., Stucchi, M., & Viganò, D. D. (2013). *Global historical earthquake archive and catalogue (1000-1903)* (GEM Technical Report 2013-01 V1.0.0) (p. 202). GEM Foundation. <https://doi.org/10.13117/GEM.GEGD.TR2013.01>
- Altunel, E., Meghraoui, M., Karabacak, V., Akyüz, S. H., Ferry, M., Yalçiner, Ç., & Munsch, M. (2009). Archaeological sites (Tell and Road) offset by the Dead Sea fault in the Amik Basin, Southern Turkey. *Geophysical Journal International*, 179(3), 1313–1329. <https://doi.org/10.1111/j.1365-246X.2009.04388.x>
- Ambraseys, N. (2009). *Earthquakes in the Mediterranean and the Middle East: A multidisciplinary study of seismicity up to 1900* (p. 947). Cambridge University Press. <https://doi.org/10.1017/CBO9781139195430>
- Ambraseys, N. N. (1988). Engineering seismology. *Earthquake Engineering & Structural Dynamics*, 17, 1–105. <https://doi.org/10.1002/eqe.4290170101>
- Ambraseys, N. N. (1989). Temporary seismic quiescence: SE Turkey. *Geophysical Journal International*, 96(2), 311–331. <https://doi.org/10.1111/j.1365-246X.1989.tb04453.x>
- Ambraseys, N. N. (2004). The 12th century seismic paroxysm in the Middle East: A historical perspective. *Annals of Geophysics*, 47, 733–758. <https://doi.org/10.4401/ag-3303>
- Ambraseys, N. N., & Barazangi, M. (1989). The 1759 earthquake in the Bekaa Valley: Implications for earthquake hazard assessment in the Eastern Mediterranean region. *Journal of Geophysical Research*, 94(B4), 4007–4013. <https://doi.org/10.1029/JB094iB04p04007>
- Ambraseys, N. N., & Finkel, C. (1987). Seismicity of Turkey and neighbouring regions 1899–1915. *Annales Geophysicae, Series B*, 5(6), 701–725.
- Ambraseys, N. N., & Finkel, C. (1995). *The seismicity of Turkey and adjacent areas: A historical review, 1500–1800* (p. 240). Eren.
- Ambraseys, N. N., & Jackson, J. A. (1998). Faulting associated with historical and recent earthquakes in the Eastern Mediterranean region. *Geophysical Journal International*, 133(2), 390–406. <https://doi.org/10.1046/j.1365-246X.1998.00508.x>
- Ambraseys, N. N., & Melville, C. P. (1995). Historical evidence of faulting in Eastern Anatolia and Northern Syria. *Annali di Geofisica*, 38(3–4), 337–343. <https://doi.org/10.4401/ag-4110>
- Barbot, S., Luo, H., Wang, T., Hamiel, Y., Piatibratova, O., Javed, M. T., et al. (2023). Slip distribution of the February 6, 2023 M_w 7.8 and M_w 7.6, Kahramanmaraş, Turkey earthquake sequence in the East Anatolian fault zone. *Seismica*, 2(3). <https://doi.org/10.26443/seismica.v2i3.502>
- Barka, A. (1996). Slip distribution along the North Anatolian fault associated with the large earthquakes of the period 1939 to 1967. *Bulletin of the Seismological Society of America*, 86(5), 1238–1254. <https://doi.org/10.1785/BSSA0860051238>
- Bayrak, E., Yılmaz, Ş., Softa, M., Türker, T., & Bayrak, Y. (2015). Earthquake hazard analysis for East Anatolian fault zone, Turkey. *Natural Hazards*, 76(2), 1063–1077. <https://doi.org/10.1007/s11069-014-1541-5>
- Bennett, R. A., Friedrich, A. M., & Furlong, K. P. (2004). Codependent histories of the San Andreas and San Jacinto fault zones from inversion of fault displacement rates. *Geology*, 32(11), 961–964. <https://doi.org/10.1130/G20806.1>
- Berryman, K. R., Cochran, U. A., Clark, K. J., Biasi, G. P., Langridge, R. M., & Villamor, P. (2012). Major earthquakes occur regularly on an isolated plate boundary fault. *Science*, 336(6089), 1690–1693. <https://doi.org/10.1126/science.1218959>
- Brown, L. (2014). *Texture shading: A new technique for depicting terrain relief* [Software]. In 9th ICA mountain cartography workshop, Banff, Canada. Retrieved from <https://app.box.com/v/textureshading>
- Carena, S., Suppe, J., & Kao, H. (2004). Lack of continuity of the San Andreas fault in southern California: 3-D fault models and earthquake scenarios. *Journal of Geophysical Research*, 109(B4), B04313. <https://doi.org/10.1029/2003JB002643>
- Çetin, H., Güneçli, H., & Mayer, L. (2003). Paleoseismology of the Palu-Lake Hazar segment of the East Anatolian fault zone, Turkey. *Tectonophysics*, 374(3–4), 163–197. <https://doi.org/10.1016/j.tecto.2003.08.003>
- Çetin, K. O., Ilgac, M., Can, G., Çakır, E., & Söylemez, B. (2020). 2020 Elazığ-Sivrice earthquake ($M_w=6.8$) reconnaissance study report (METU/EERC 2020-01). Middle East Technical University.
- Daëron, M., Klinger, Y., Tapponnier, P., Elias, A., Jacques, E., & Sursock, A. (2007). 12,000-year-long record of 10 to 13 paleo-earthquakes on the Yammouneh fault, Levant fault system, Lebanon. *Bulletin of the Seismological Society of America*, 97(3), 749–771. <https://doi.org/10.1785/0120060106>
- Darawceh, R., Abdul-Wahed, M. K., & Hasan, A. (2022). The Great 1822 Aleppo Earthquake: New historical sources and strong ground motion simulation. *Geofisica Internacional*, 61(3), 201–228. <https://doi.org/10.22201/igeof.00167169p.2022.61.3.2198>
- Duman, T. Y., & Emre, Ö. (2013). The East Anatolian fault: Geometry, segmentation and jog characteristics. In A. H. F. Robertson, O. Parlak, & U. C. Ünlügenç (Eds.), *Geological development of Anatolia and the easternmost Mediterranean region* (p. 372). Geological Society, London, Special Publications. <https://doi.org/10.1144/SP372.14>
- European Space Agency, & Sinergise. (2021). Copernicus global digital elevation model [Dataset]. <https://doi.org/10.5270/ESA-c5d3d65>
- ForM@Ter—EOST. (2023). Terrain displacement from the Türkiye-Syria earthquakes of February 6, 2023 obtained with the GDM-OPT-ETQ service applied on Sentinel-2 optical imagery [Dataset]. <https://doi.org/10.25577/EWT8-KY06>
- Friedrich, A. M., Wernicke, B. P., Niemi, N. A., Bennett, R. A., & Davis, J. L. (2003). Comparison of geodetic and geologic data from the Wasatch region, Utah, and implications for the spectral character of Earth deformation at periods of 10 to 10 million years. *Journal of Geophysical Research*, 108(B4), 2199. <https://doi.org/10.1029/2001JB000682>
- Gasperini, P., & Ferrari, G. (2000). Deriving numerical estimates from descriptive information: The computation of earthquake parameters. *Annali di Geofisica*, 43(4), 729–746. <https://doi.org/10.4401/ag-3670>
- Guidoboni, E., Bernardini, F., & Comastri, A. (2004). The 1138–1139 and 1156–1159 destructive seismic crises in Syria, South-Eastern Turkey and northern Lebanon. *Journal of Seismology*, 8(1), 105–127. <https://doi.org/10.1023/B:JOSE.0000009502.58351.06>
- Guidoboni, E., Bernardini, F., Comastri, A., & Boschi, E. (2004). The large earthquake on 29 June 1170 (Syria, Lebanon, and central southern Turkey). *Journal of Geophysical Research*, 109(B7), B07304. <https://doi.org/10.1029/2003JB002523>
- Guidoboni, E., & Comastri, A. (2005). *Catalogue of earthquakes and tsunamis in the Mediterranean area from the 11th to the 15th century* (p. 1037). INGV-SGA.

- Guidoboni, E., Ferrari, G., Mariotti, D., Comastri, A., Tarabusi, G., Sgattoni, G., et al. (2018). *CFT15Med, Catalogo dei Forti Terremoti in Italia (461 a.C.-1997) e nell'area Mediterranea (760 a.C.-1500)*. Istituto Nazionale di Geofisica e Vulcanologia (INGV). <https://doi.org/10.6092/ingv.it-cft15>
- Guidoboni, E., Ferrari, G., Tarabusi, G., Sgattoni, G., Comastri, A., Mariotti, D., et al. (2019). CFT15Med, the new release of the catalogue of strong earthquakes in Italy and in the Mediterranean area. *Scientific Data*, 6(1), 80. <https://doi.org/10.1038/s41597-019-0091-9>
- Gülerce, Z., Tanvir Shah, S., Menekşe, A., Arda Özacar, A., Kaymakci, N., & Önder Çetin, K. (2017). Probabilistic seismic-hazard assessment for East Anatolian fault zone using planar fault source models. *Bulletin of the Seismological Society of America*, 107(5), 2353–2366. <https://doi.org/10.1785/0120170009>
- Gürboğa, S., & Gökçe, O. (2019). Paleoseismological catalog of Pre-2012 trench studies on the active faults in Turkey. *Bulletin of Mineral Research and Exploration*, 159, 63–87. <https://doi.org/10.19111/bulletinofmre.561925>
- Güvercin, S. E., Karabulut, H., Konca, A. Ö., Doğan, U., & Ergintav, S. (2022). Active seismotectonics of the East Anatolian fault. *Geophysical Journal International*, 230(1), 50–69. <https://doi.org/10.1093/gji/ggac045>
- Hubert-Ferrari, A., Barka, A., Jacques, E., Nalbant, S. S., Meyer, B., Armijo, R., et al. (2000). Seismic hazard in the Marmara Sea region following the 17 August 1999 Izmit earthquake. *Nature*, 404(6775), 269–273. <https://doi.org/10.1038/35005054>
- Hubert-Ferrari, A., King, G., Manighetti, I., Armijo, R., Meyer, B., & Tapponnier, P. (2003). Long-term elasticity in the continental lithosphere; modelling the Aden Ridge propagation and the Anatolian extrusion process. *Geophysical Journal International*, 153(1), 111–132. <https://doi.org/10.1046/j.1365-246X.2003.01872.x>
- Hubert-Ferrari, A., Lamair, L., Hage, S., Schmidt, S., Çağatay, M. N., & Avsar, U. (2020). A 3800 yr paleoseismic record (Lake Hazar sediments, eastern Turkey): Implications for the East Anatolian fault seismic cycle. *Earth and Planetary Science Letters*, 538, 11615. <https://doi.org/10.1016/j.epsl.2020.116152>
- Karakhanian, A. S., Trifonov, V. G., Ivanova, T. P., Avagyan, A., Rukieh, M., Minini, H., et al. (2008). Seismic deformation in the St. Simeon Monasteries (Qal'at Sim'an), Northwestern Syria. *Tectonophysics*, 453(1–4), 122–147. <https://doi.org/10.1016/j.tecto.2007.03.008>
- Khair, K., Karakaisis, G. F., & Papadimitriou, E. (2000). Seismic zonation of the Dead Sea transform fault area. *Annali di Geofisica*, 43(1), 61–79. <https://doi.org/10.4401/ag-3620>
- King, G. C. P., Stein, R. S., & Lin, J. (1994). Static stress changes and the triggering of earthquakes. *Bulletin of the Seismological Society of America*, 84, 935–953. <https://doi.org/10.1785/BSSA0840030935>
- Kondorskaya, R. N. V., & Ulomov, V. I. (1999). *Special catalogue of earthquakes of Northern Eurasia (SECNE) from ancient times through 1995*. Joint Institute of Physics of the Earth (JIPE), Russian Academy of Sciences.
- Lefevre, M., Klinger, Y., Al-Qaryouti, M., Le Béon, M., & Moumani, K. (2018). Slip deficit and temporal clustering along the Dead Sea fault from paleoseismological investigations. *Scientific Reports*, 8(1), 4511. <https://doi.org/10.1038/s41598-018-22627-9>
- Marco, S., & Klinger, Y. (2014). Review of on-fault palaeoseismic studies along the Dead Sea fault. In *Dead Sea transform fault system: Reviews* (pp. 183–205). https://doi.org/10.1007/978-94-017-8872-4_7
- McCaffrey, R. (2008). Global frequency of magnitude 9 earthquakes. *Geology*, 36(3), 263–266. <https://doi.org/10.1130/G24402A.1>
- Meghraoui, M. (2015). Paleoseismic history of the Dead Sea fault zone. In M. Beer, I. A. Kougioumtzoglou, E. Patelli, & I. S.-K. Au (Eds.), *Encyclopedia of earthquake engineering*. Springer-Verlag Berlin. https://doi.org/10.1007/978-3-642-36197-5_40-1
- Meghraoui, M., Gomez, F., Sbeinati, R., Van der Woerd, J., Mouty, M., Darkal, A. N., et al. (2003). Evidence for 830 years of seismic quiescence from palaeoseismology, archaeoseismology and historical seismicity along the Dead Sea fault in Syria. *Earth and Planetary Science Letters*, 210(1–2), 35–52. [https://doi.org/10.1016/S0012-821X\(03\)00144-4](https://doi.org/10.1016/S0012-821X(03)00144-4)
- Ou, Q., Lazecky, M., Watson, C. S., Maghsoudi, Y., & Wright, T. (2023). 3D displacements and strain from the 2023 February Turkey earthquakes version 1 [Dataset]. NERC EDS Centre for Environmental Data Analysis. <https://doi.org/10.5285/df93e92a3adc46b9a5c4bd3a547cd242>
- Öztürk, S. (2021). Spatio-temporal analysis on the aftershocks of January 24, 2020, Mw6.8 Sivrice-Elazığ (Turkey) Earthquake. In *PACE-2021 international congress on the phenomenological aspects of civil engineering, 20–23 June 2021*. Atatürk University. Paper 364.
- Papathanassiou, G., Pavlides, S., Christaras, B., & Ptilakis, K. (2005). Liquefaction case histories and empirical relations of earthquake magnitude versus distance from the broader Aegean region. *Journal of Geodynamics*, 40(2–3), 257–278. <https://doi.org/10.1016/j.jog.2005.07.007>
- Perinçek, D., & Çemen, I. (1990). The structural relationship between the East Anatolian and Dead Sea fault zones in southeastern Turkey. *Tectonophysics*, 172(3–4), 331–340. [https://doi.org/10.1016/0040-1951\(90\)90039-B](https://doi.org/10.1016/0040-1951(90)90039-B)
- Philibosian, B., & Meltzner, A. J. (2020). Segmentation and supercycles: A catalog of earthquake rupture patterns from the Sumatran Sunda Megathrust and other well-studied faults worldwide. *Quaternary Science Reviews*, 241, 106390. <https://doi.org/10.1016/j.quascirev.2020.106390>
- Pousse-Beltran, L., Nissen, E., Bergman, E. A., Cambaz, M. D., Gaudreau, É., Karasözen, E., & Tan, F. (2020). The 2020 M_w 6.8 Elazığ (Turkey) earthquake reveals rupture behavior of the East Anatolian fault. *Geophysical Research Letters*, 47(13), e2020GL088136. <https://doi.org/10.1029/2020GL088136>
- Reitman, N. G., Briggs, R. W., Barnhart, W. D., Thompson Jobe, J. A., DuRoss, C. B., Hatem, A. E., et al. (2023). Preliminary fault rupture mapping of the 2023 M_w 7.8 Türkiye Earthquakes [Dataset]. <https://doi.org/10.5066/P98517U2>
- Rosakis, A., Abdelmeguid, M., & Elbanna, A. (2023). Evidence of early supershear transition in the M_w 7.8 Kahramanmaraş earthquake from near-field records. EarthArXiv [preprint]. <https://doi.org/10.31223/X5W95G>
- Rukieh, M., Trifonov, V. G., Dodonov, A. E., Minini, H., Ammar, O., Ivanov, T. P., et al. (2005). Neotectonic map of Syria and some aspects of Late Cenozoic evolution of the northwestern boundary zone of the Arabian plate. *Journal of Geodynamics*, 40(2–3), 235–256. <https://doi.org/10.1016/j.jog.2005.07.016>
- Salamon, A. (2008). *Patterns of aftershock sequences along the Dead Sea transform - Interpretation of historical seismicity* (Report GSI/05/2008) (p. 78). Geological Survey of Israel.
- Salditch, L., Stein, S., Neely, J., Spencer, B. D., Brooks, E. M., Agnon, A., & Liu, M. (2020). Earthquake supercycles and long-term fault memory. *Tectonophysics*, 774, 228289. <https://doi.org/10.1016/j.tecto.2019.228289>
- Satılmış, S. (2016). 1893 Malatya Earthquake and Disaster Management. *Journal of the Center for Ottoman Studies Ankara University*, 39, 137–177.
- Sbeinati, M. R., Darawch, R., & Mouty, M. (2005). The historical earthquakes of Syria: An analysis of large and moderate earthquakes from 1365 B.C. to 1900 A.D. *Annals of Geophysics*, 47, 733–758.
- Sbeinati, M. R., Meghraoui, M., Suleyman, G., Gomez, F., Grootes, P., Nadeau, et al. (2010). Timing of earthquake ruptures at the Al Harif Roman aqueduct (Dead Sea fault, Syria) from archaeoseismology and paleoseismology. In M. Sintubin, I. S. Stewart, T. M. Niemi, & E. Altunel (Eds.), *Ancient earthquakes: Geological Society of America Special Paper 471* (pp. 243–267). [https://doi.org/10.1130/2010.2471\(20](https://doi.org/10.1130/2010.2471(20)
- Scordilis, E. M. (2006). Empirical global relations converting M_s and mb to moment magnitude. *Journal of Seismology*, 10(2), 225–236. <https://doi.org/10.1007/s10950-006-9012-4>

- Seyrek, A., Demir, T., Pringle, M. S., Yurtmen, S., Westaway, R. W. C., Beck, A., et al. (2007). Kinematics of the Amanos fault, southern Turkey, from Ar/Ar dating of offset Pleistocene basalt flows: Transpression between the African and Arabian plates. In W. D. Cunningham & P. Mann (Eds.), *Tectonics of strike-slip restraining and releasing bends* (Vol. 290, pp. 255–284). Geological Society, London, Special Publications. <https://doi.org/10.1144/SP290.9>
- Seyrek, A., Demir, T., Westaway, R., Guillou, H., Scaillet, S., White, T. S., & Bridgland, D. R. (2014). The kinematics of central-southern Turkey and northwest Syria revisited. *Tectonophysics*, *618*, 35–66. <https://doi.org/10.1016/j.tecto.2014.01.008>
- Stein, R. S., Barka, A. A., & Dieterich, J. H. (1997). Progressive failure on the North Anatolian fault since 1939 by earthquake stress triggering. *Geophysical Journal International*, *128*(3), 594–604. <https://doi.org/10.1111/j.1365-246X.1997.tb05321.x>
- Taftoglou, M., Valkaniotis, S., Karantanellis, E., Goula, E., & Papathanassiou, G. (2023). Preliminary mapping of liquefaction phenomena triggered by the February 6 2023 M7.7 earthquake, Türkiye/Syria, based on remote sensing data. *Zenodo*. <https://doi.org/10.5281/zenodo.7668400>
- Tozer, B., Sandwell, D. T., Smith, W. H. F., Olson, C., Beale, J. R., & Wessel, P. (2019). Global bathymetry and topography at 15 Arc Sec: SRTM15+ [Dataset]. *Earth and Space Science*, *6*(10), 1847–1864. <https://doi.org/10.1029/2019EA000658>
- U.S. Geological Survey. (2023). Earthquake lists, maps, and statistics. Retrieved from <https://www.usgs.gov/natural-hazards/earthquake-hazards/lists-maps-and-statistics>
- Wan, Y., Shen, Z.-K., Bürgmann, R., Sun, J., & Wang, M. (2017). Fault geometry and slip distribution of the 2008 M_w 7.9 Wenchuan, China earthquake, inferred from GPS and InSAR measurements. *Geophysical Journal International*, *208*(2), 748–766. <https://doi.org/10.1093/gji/ggw421>
- Wells, D. L., & Coppersmith, K. J. (1994). New empirical relationships among magnitude, rupture length, rupture width, rupture area, and surface displacement. *Bulletin of the Seismological Society of America*, *84*(4), 974–1002. <https://doi.org/10.1785/BSSA0840040974>
- Wessel, P., Luis, J. F., Uieda, L., Scharroo, R., Wobbe, F., Smith, W. H. F., & Tian, D. (2019). The Generic Mapping Tools version 6. *Geochemistry, Geophysics, Geosystems*, *20*(11), 5556–5564. <https://doi.org/10.1029/2019GC008515>
- Westaway, R. (2004). Kinematic consistency between the Dead Sea fault zone and the Neogene and Quaternary left-lateral faulting in SE Turkey. *Tectonophysics*, *391*(1–4), 203–237. <https://doi.org/10.1016/j.tecto.2004.07.014>
- Yönlü, Ö. (2012). Late Quaternary activity of the east Anatolian fault zone between Gölbasi (Adiyaman) and Karataş (Adana) (Doctoral dissertation). Dept. of Geological Engineering, Eskişehir Osmangazi Üniversitesi (In Turkish).
- Zelenin, E., Bachmanov, D., Garipova, S., Trifonov, V., & Kozhurin, A. (2022). The Active Faults of Eurasia Database (AFEAD): The ontology and design behind the continental-scale dataset [Dataset]. *Earth System Science Data*, *14*(10), 4489–4503. <https://doi.org/10.5194/essd-14-4489-2022>